Beni-Suef University Journal of Basic and Applied Sciences

REVIEW

Open Access

Nanotoxicological profiles of clinically approved nanoplatforms

Christian Isalomboto Nkanga[1*]

Abstract

Background Nanoparticles (NPs) engineering offers great opportunities to produce versatile materials for multiple applications in medicine, including drug delivery and bioimaging. Successful development of nanomedicines up to the clinical level is evidence that nanotechnology has made gigantic strides in addressing health problems.

Area covered This review briefly discusses the toxicological data from selected clinically relevant nanoplatform technologies (i.e. liposomes, poly(lactide-*co*-glycolide) and iron oxide NPs); comparisons between such nano-systems provide insights into existing challenges in nanotoxicity assessment. The factors that can affect nanoparticles toxicity have been discussed as well. Albeit most studies reported no major toxicological effects, the analysis of reported data pinpoints the lack of organ-function studies as well as the difficulty in comparing nanotoxicity findings from different protocols due to the discrepancies in experimental conditions.

Conclusion The previously developed nanomedicines are likely a result of constant efforts dedicated to improving the quality attributes of individual products on case-by-case basis, given the luck of design rules for optimal nanoproducts. Thus, further systematic investigations are required to streamline the general design principles in nanoproducts development and boost the translation of NPs from bench to bedside.

Keywords Nanoscale, Nanostructure, Chemical composition, Biomaterial, Biomedicine, Toxicity

1 Background

Nanotechnology offers great opportunities for the transformation of materials from bulk to particulate state, in which most of the material components (i.e. nanoparticles) have sizes at the nanometric scale (below 100 nm). Nanosized materials distinctly exhibit higher surface to volume ratios and impressive physicochemical and electromechanical properties useful in different fields of science and technology [68]. Efforts in nanoengineering have thrived to produce valuable nanoparticles (NPs) for various applications across different sectors, such as energy, agriculture and biomedicine. In biomedicine, the nanometric regime of NPs is an asset because most of the biological structures (e.g. proteins and DNA) operate at the same size scale. This underlines the growing applications of NPs in medicine, particularly in the field of bioimaging for diagnosis [69], drug delivery [14], immunotherapy [124] and vaccine development [124]. The use of NPs in medicine (i.e. nanomedicine) has made enormous strides in addressing health problems through effective drug development from the bench to the bedside. As recently discussed in the reviews by Anselmo and Mitragotri [8] and Zhong et al. [159], there are NPs-based products in clinical trials, and up to 30 nanomedicines in the pharmaceutical market. With the outbreak of the severe acute respiratory syndrome coronavirus 2 (SARS-CoV-2), these statistics have drastically changed due to the urgent COVID-19 vaccine development. There are up to 20 NPs-based vaccines already approved in the clinic, and more than 100 candidates are in clinical trials [28].

*Correspondence:
Christian Isalomboto Nkanga
christian.nkanga@unikin.ac.cd
[1] Department of Medicinal Chemistry and Pharmacognosy, Faculty of Pharmaceutical Sciences, University of Kinshasa, B.P. 212, Kinshasa XI, Democratic Republic of the Congo

Notably, the ability of nanoengineered materials to perform at the nanometric scale is a double-edged sword: while they are desired to provide new solutions to disease shortcomings, they can be detrimental to normal physiological functions or anatomical structures, if not optimized accordingly. For instance, Kolosnjaj-Tabi et al. [72] demonstrated that the nanosized components of inhaled particulate matters (i.e. carbon nanotubes) from air pollution are responsible for lung impairment. Another study reported the crucial contribution of nanometric size as a key element of cytotoxicity: while 20–80 nm silver (Ag) NPs were predicted to be cytotoxic due to high Ag ions release loads, 10 nm AgNPs were found to be way more cytotoxic because of their higher intracellular bioavailability [63]. There are other parameters (such as shape, surface charge and coating) that raise concern in nanotechnology as they increase the accessibility and reactivity of NPs towards the biological structures. With the growing use of biomaterials in nanotechnology, the intrinsic composition of biomedical NPs remains at the heart of development; efforts are often made so that the by-products from NPs degradation appear in biogenic forms [146]. This is a critical element of biosafety since the similarity with endogenous compounds may set the stage for good biocompatibility, but one big concern is the difficulty to distinguish metabolites from NPs degradation *versus* endogenous metabolites [120]. Nonetheless, formulation scientists are committed to continuously improving the biosafety profiles of NPs and boosting their clinical translation.

The fact that nanomedicine has delivered clinically relevant nanoplatform technologies into the pharmaceutical market is a considerable stride, likely arising from dedicated efforts to improve the quality attributes of individual products, but it is not a reflection of successful implementation of general design rules for the development of ideal nanoproducts. The gap between NPs product output and research input clearly shows the existence of high technical barriers hindering clinical translation, which is seen in the low number of NPs formulations entering the market *versus* increasing loads of research publications [159]. The lack of unified protocols for NPs evaluation is among the bottlenecks that hold nanomedicine from unfolding fully [154, 156]. The limitations in NPs testing have been recently reviewed [84].

This review briefly discusses the toxicological considerations pertaining to some of the nanoplatforms currently used in the clinic. Based on their inherent biodegradability, the platforms selected for this review include liposomes, poly(lactide-*co*-glycolide) (PLGA) and iron oxide NPs (IONPs), as representative illustrations of lipid-based, polymeric and metallic systems, respectively. The structural organization, biological fates, nanoparticulate properties and key data related to nanotoxicity of these platforms have been discussed.

2 Main text

2.1 Structural organization of nanoplatforms

The platform nanotechnologies explored in this review have distinct chemical compositions, being made up of phospholipids (liposomes), polymer (PLGA) and metal oxide (IONPs) (Fig. 1). The following paragraphs briefly highlight the structural organization of each platform to establish the fundamental differences that set them apart and may likely be one of the reasons for the differences in their nanotoxicological profiles.

2.1.1 Liposomes

Liposomes are artificial vesicular particles mainly composed of phospholipids, which are amphiphilic compounds naturally found in the cell membranes. Due to their compartmental structure, with a lipophilic membrane enclosing an aqueous core, liposomes offer the advantage of encapsulating molecular cargoes of hydrophilic, amphiphilic and hydrophobic natures (Fig. 1A). Liposomes are made of one or more phospholipid bilayers and produced in a diverse range of sizes, from 20 nm to several micrometres [98], as shown in Fig. 2A, B. The versatility of liposomes in the encapsulation processes has been demonstrated. They are reputed to be smart vehicles for molecular species of variable structure, from small and simple to large and complex molecules [45, 100, 113, 142]. In addition, the ease of surface modification enables the development of liposomes with multiple functionalities, such as stealth, long-circulating and ligand targeting properties [36]. These features set the basis for the applications of liposomes across various areas of nanomedicine, including site-specific drug delivery [17], non-invasive imaging techniques like magnetic resonance imaging (MRI) soft tissue morphological imaging and positron emission tomography (PET) [76] and immunotherapy [60].

2.1.2 PLGA systems

PLGA is a family of FDA-reputed co-polyesters of lactic acid (LA) with glycolic acid (GA) at various LA/GA ratios. Due to their excellent mechanical and processing characteristics, PLGA systems have been widely used for various biomedical applications, such as advanced drug delivery (i.e. sustained release, targeted delivery and protection of drug molecules), tissue engineering and regeneration medicine [90]. Depending on the cargo's properties, PLGA-based architectures achieve drug product encapsulation through molecular or particulate (micronized solid) dispersion within the polymeric matrix [44], as illustrated in Fig. 1B. The types of

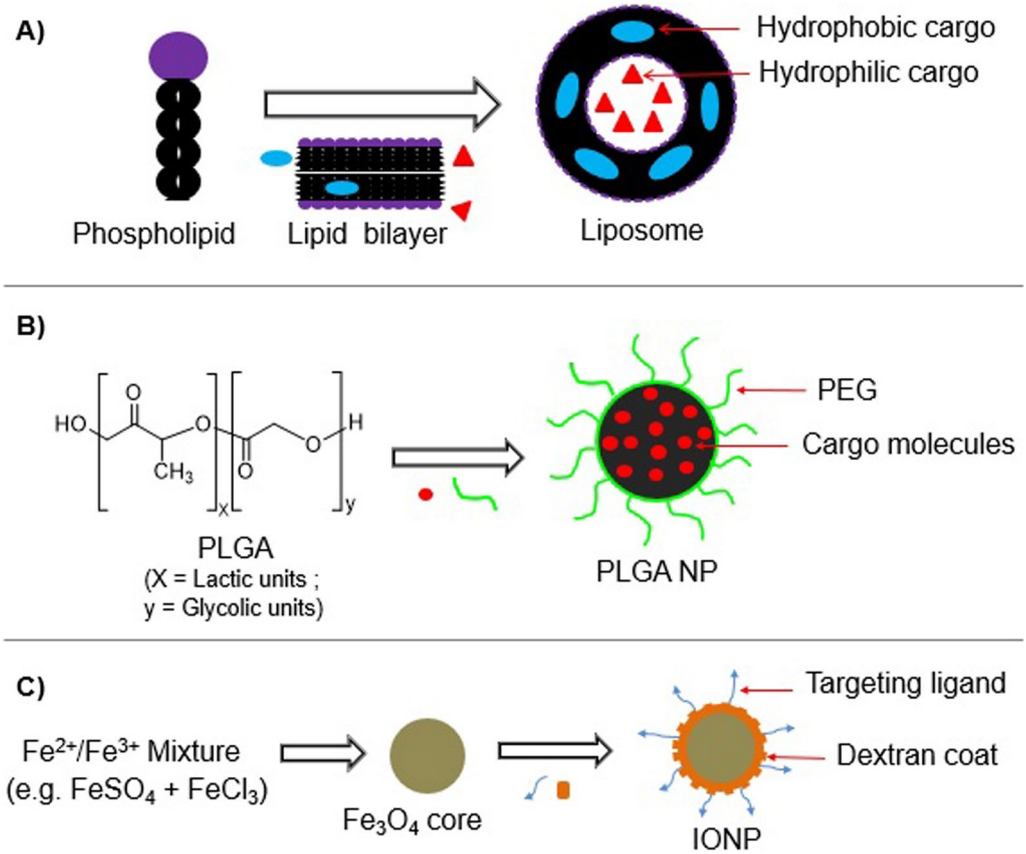

Fig. 1 Schematic representation of clinically approved synthetic nanoplatforms: **A** showing liposome formation and cargo encapsulation; **B** illustrating the formation of laden PLGA NPs decorated with stealth polymers (PEG); **C** illustrative formation of IONPs made of iron oxide (Fe_3O_4) core coated with carbohydrates (dextran) and decorated with targeting ligands

cargoes vary from small drug molecules to macromolecules such as proteins and nucleic acids [134]. One of the most attractive features of PLGA systems is the tuneable release characteristics, which can be adjusted to afford long-acting dosage forms for improved patient compliance. Since the ester bonds of PLGA are subject to in vivo hydrolysis (*i.e.* esterase-mediated digestion), the release kinetics of drug molecules is mainly driven by polymer biodegradation and erosion [39]. Consequently, critical factors controlling drug release rates encompass the polymer molecular weight, LA/GA ratio and size and shape of the matrix. PLGA nanoparticles can exhibit various size patterns depending on the formulation treatments (Fig. 2C, D). Owing to the contribution of drug diffusion rate, additional parameters such as loading capacity, end terminus of polymer (e.g. acid terminated or ester terminated) and drug-polymer interactions have also been identified as key to release kinetics [66]. Drug release characteristics are part of the clinically relevant factors governing PLGA-based product efficacy and safety profiles [105], since PLGA copolymers are reputed biomaterials with commendable biocompatibility, as demonstrated by the existence of several clinically approved PLGA-based formulations [99].

2.1.3 Iron oxide nanoparticles

Iron oxide nanoparticles (IONPs) are one of the privileged ferromagnetic materials endowed with superparamagnetism, which makes them attractive for various sectors, including medicine and biology [4]. Among the types of iron oxides—namely magnetite (Fe_3O_4), maghemite (γ-Fe_2O_3) and wüstite (FeO), magnetite exhibits the optimal ferrimagnetism and highest saturation magnetization [152]. Owing to their excellent superparamagnetic properties and small size characteristics (Fig. 2E, F), IONPs with magnetite core, often referred to as superparamagnetic nanoparticles (SPIONs), have been extensively investigated for several biomedical applications, encompassing diagnostic magnetic resonance imaging (MRI), magnetic photothermal therapy and drug delivery [15, 37, 42, 115]. SPIONs are one of the few FDA-approved nanomedicines for clinical uses.

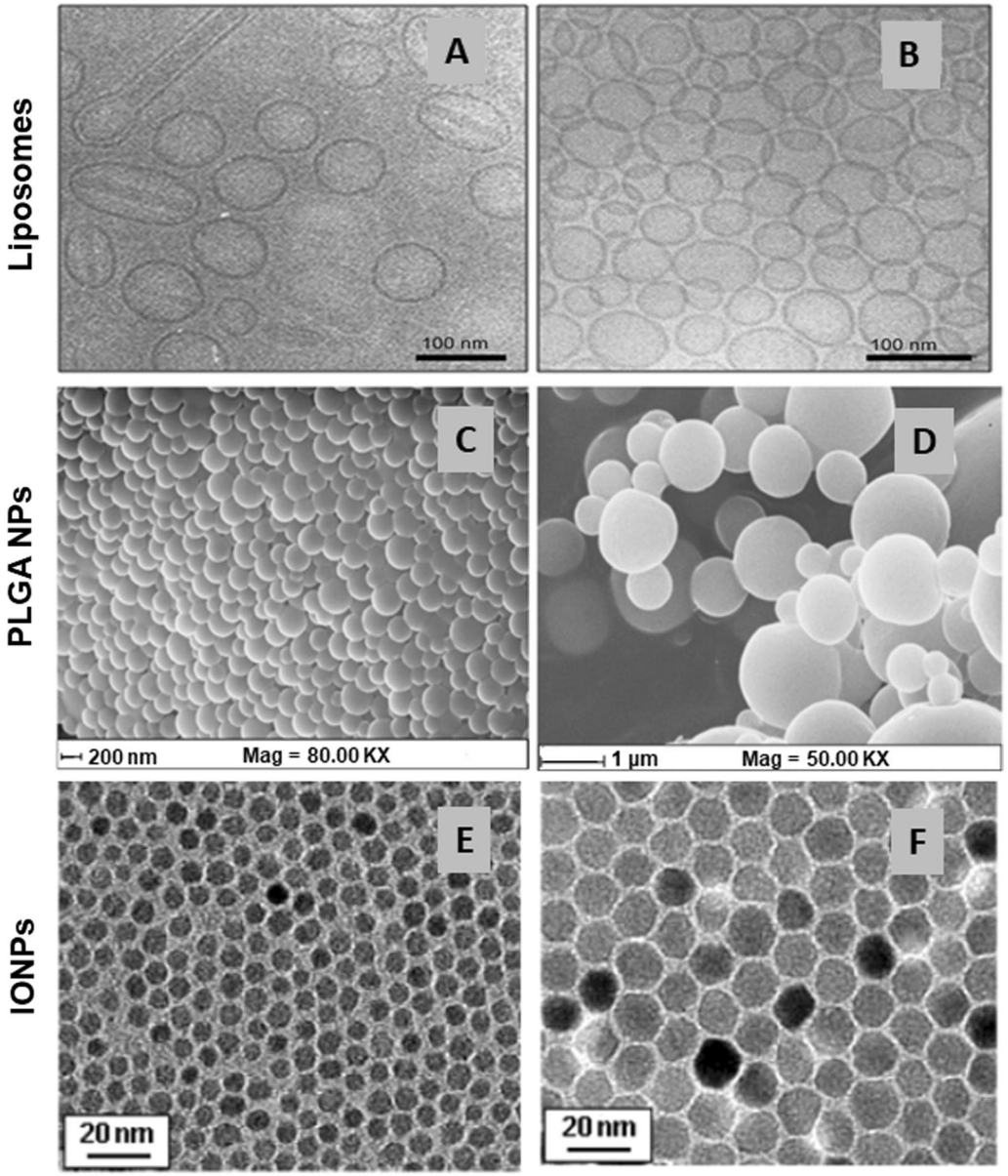

Fig. 2 Micrographs illustrating the nanoscale regime of nanoplatforms discussed herein. Cryogenic transmission electron microscopy (TEM) of liposomes loaded with doxorubicin (**A**) and cisplatin (**B**)—Reprinted from [136], with permission from Elsevier (licence number 5667521309110). Scanning electron microscopy (SEM) of PLGA NPs after freeze-drying (**C**) and spray-drying (**D**)—Reprinted from [123], with permission from Elsevier (licence number 5667530389172). TEM images of 6 nm (**E**) versus 12 nm (**F**) IONPs—Reprinted and adapted with permission from [121]. Copyright 2004 American Chemical Society

Examples of marketed SPION products include Feridex® [21], Feraheme® [141] and NanoTherm® [119], which are used for liver MRI, iron deficiency and local hyperthermia tumour therapy, respectively. As shown in Fig. 1C, an essential constituent of SPIONs for successful biomedical applications is the surface coat from particle functionalization [95], which is mostly made of hydrophilic biomaterials such as carbohydrates [3, 85]. The ability to biofunctionalize SPIONs laid the foundation for controlling their biological fate, ensuring optimal in vivo performance [27]. For instance, this allows for imparting targeting capabilities or addressing protein corona formation to improve bioavailability [131].

2.2 NPs fates and nanotoxicity profiles

2.2.1 Overview of NPs fates

The increasing use of NPs in biomedicine has motivated continuous efforts to understand their behaviour and fates in biological systems. Many studies have highlighted the relevance of the characteristics of NPs (e.g. particle size, shape and charge) as intrinsic factors that dictate the fates of NPs. However, there are also numerous extrinsic parameters such as administration routes, pharmacokinetics and biodistribution that play pivotal roles [59, 133]. Many of these NPs-unrelated factors depend on various barriers, which stem from the normal physiology/anatomy, pathology and cell mechanisms. These barriers can either grant NPs access to or block them from certain biological areas or functions (Fig. 3). Such barriers can tip the balance between nanotoxicological and nanotherapeutic effects [91]. Therefore, a deeper understanding of the interactions between NPs and biological barriers is crucial for designing effective NPs with minimized side effects.

Regardless of the targeting features, NPs distribute across various tissues and organs. Their distribution is influenced by factors such as the route of administration, the intrinsic properties of NPs and physiological and pathological conditions [52]. Consequently, different concentrations of NPs can be detected in various organs [79]. Irrespective of the administration routes, NPs eventually enter the bloodstream [81, 156], making their potential impact on the blood (haematotoxicity) a focus in nanotoxicity studies. Additionally, the formation of protein corona on NPs surfaces is commonly considered as a key determinant of their behaviour in the body. This corona affects biodistribution, accumulation and clearance of NPs [6] and essentially determines

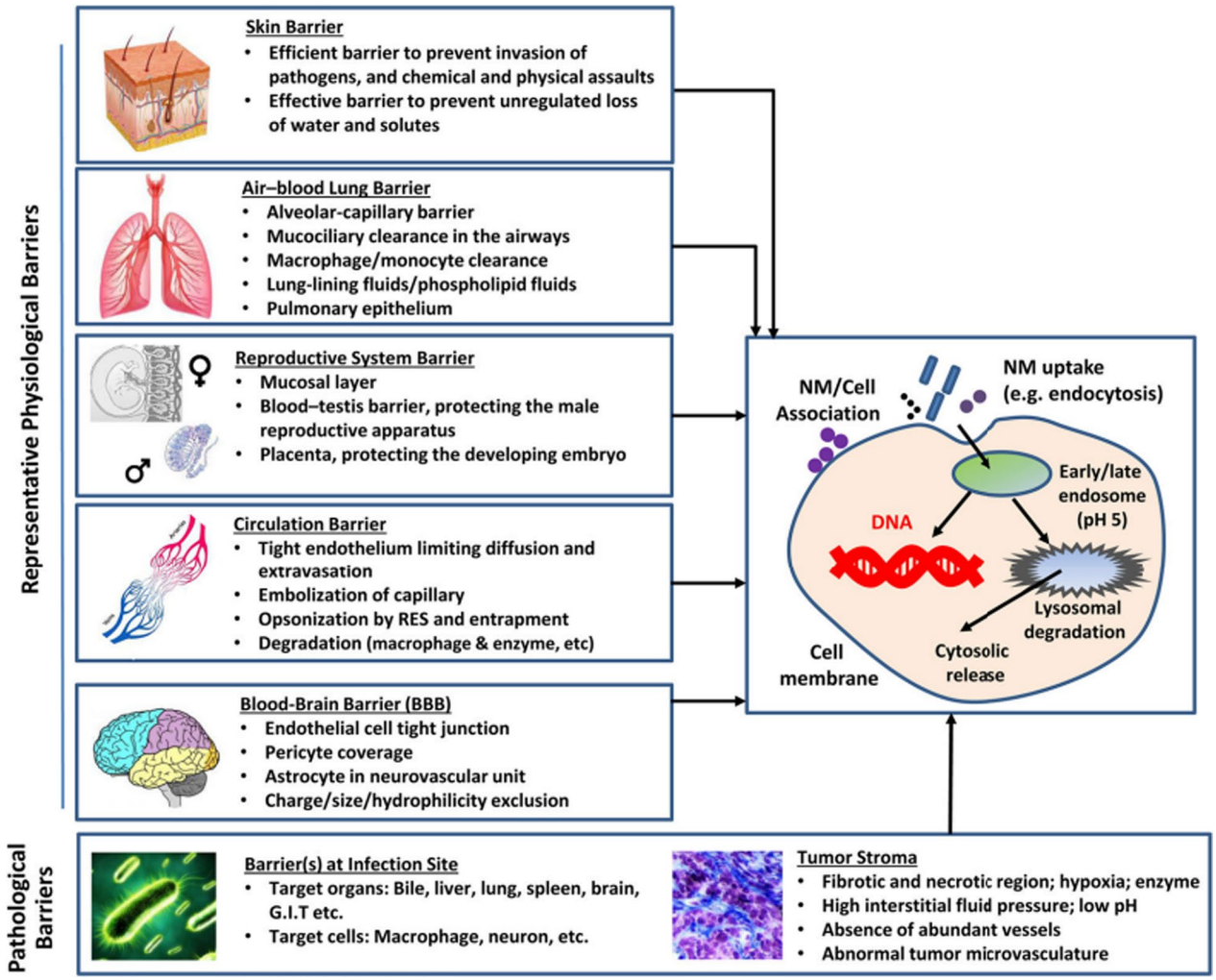

Fig. 3 Schematic illustrations of naturally occurring and pathological barriers that can affect the fates of NPs in the body. Reproduced from Meng et al. [91], with permission from Elsevier (licence number 5373331323566)

their biological identity in vivo. Notably, the composition of protein corona greatly influences the fate of NPs. For instance, when the corona is mainly made of opsonins, such as complement proteins and immunoglobulins, it aids in the NPs' quick recognition and uptake by phagocytic cells [2, 102].

In addition to the plasma clearance resulting from protein corona formation, off-target tissue accumulation of NPs is a concerning issue that can reduce their efficacy and increase side effects. Factors driving off-target biodistribution include uptake by immune cells and tissue entrapment through endothelial fenestrations [43]. On the one hand, the phagocytic cells like monocytes and macrophages influence the ultimate organ accumulation patterns of NPs due to their localization in the body. While these immune cells are ubiquitous, they are primarily found in the liver, spleen, bone marrow and lymph nodes. These organs collectively constitutes the monocyte-macrophage cell system, also called the reticuloendothelial system (RES). Consequently, intensive phagocytosis of NPs by immune cells leads to their sequestration and accumulation in the RES organs [83].

On the other hand, the endothelium fenestrations in some tissues (e.g. liver, spleen, kidney and tumour tissues) have a direct impact on the organ distribution and accumulation of NPs [43]. While pathological fenestrations (as found in tumour tissues) favour passive targeting through the enhanced permeability and retention effect [53, 145], naturally occurring fenestrated endothelia found in the RES organs cause off-target accumulation of NPs, potentially leading to adverse side effects. The liver is the primary component of the RES and comprises both RES cells (i.e. liver macrophages, called Kupffer cells) and non-RES hepatic cells. This dual composition leads to two potential destinies for NPs within the liver: either clearance through bile when engulfed by non-RES cells or retention within the hepatic tissue following phagocytosis by Kupffer cells [83]. In the spleen, the phagocytic cells play a role in the organ's filtration function, trapping undesired cells (such as ageing red blood cells) and foreign particles like NPs within the splenic tissue. Given the inevitable sequestration by the RES organs, histopathological and biochemical characterizations, as well as organ-function studies, become crucial for nanotoxicity evaluations. This helps ensure that the NPs designed for medical applications are both biocompatible and effective [26, 75, 154].

2.2.2 Nanotoxicological profiles of selected platforms

In vitro screening frequently serves as the first line of nanotoxicity screening, aiding in determining the minimum toxic dose to predict in vivo nanotoxicity [122]. Techniques for this in vitro nanotoxicity assessment typically encompass cell viability assays—subdivided into categories such as cell proliferation, necrosis and apoptosis tests. Additionally, investigations into cytotoxicity mechanisms, like the exploration of oxidative stress and DNA damage are also pivotal in these assessments [154]. In vitro nanotoxicity data primarily serve for guidance [65]. Yet, extrapolating these findings to an in vivo context can pose challenges due to the extremes of in vitro conditions, such as the use of ultra-high doses and extended exposure durations during dose-related cytotoxicity assessments [156]. Therefore, in vivo assessments are recognized as a pertinent and comprehensive method to evaluate nanotoxicity. However, they are also acknowledged as intricate, necessitating animal sacrifice and being time-intensive [154]. I*n vivo* nanotoxicity evaluations mostly focus on histopathological alterations, in addition to analysing various biological and biochemical markers, including haematology, cellular metabolism and clearance mechanisms [26, 75]. The subsequent subsections provide a concise overview of significant in vitro and in vivo nanotoxicity data associated with liposomes, PLGA systems and IONPs.

2.2.2.1 Liposomes The medical use of liposomes takes advantage of their nanometric functionalities, but also the possibility of developing different dosage forms for any routes of administration depending on the expected efficacy and safety, as demonstrated by the marketed products [20]. In fact, being made of naturally occurring biodegradable lipids (phospholipids), liposomes are part of materials commonly reputed to have high biocompatibility profiles. This can be illustrated by the phospholipid mixtures (i.e. Beractant, Survanta®) currently commercialized as artificial lung surfactants for prophylaxis treatment of the respiratory distress syndrome in neonates [110, 118]. However, when used as a delivery system, liposomes exhibit variable safety profiles depending not only on the formulation composition but also on the vesicles behaviour in vivo (i.e. biodistribution patterns).

There are many insightful studies illustrating the liposome's potential to impact the overall safety profile of a therapeutic nano-formulation (Table 1) positively or negatively. The liposomal particle's inherent factors (such as size and surface charge) have been tuned to control the in vivo fate of liposomes for improved product biocompatibility. For instance, Charrois and Allen investigated the impact of the diameter of liposomes on doxorubicin's pharmacokinetics and biodistribution to minimize drug cutaneous toxicity while enhancing tumour homing [24]. The differences in the time courses of liposome accumulation in the tumour, skin and paws tissues were obvious, but no preferential accumulation into the tumour tissues was achieved. The influence of surface charge

Table 1 Summary of representative studies evaluating the biocompatibility and toxicity of liposomes

Formulation composition	Preparation method	Liposome dose (administration route)	Animal/cell type	Cell/tissue target	Biocompatibility-/toxicity-related outcomes	References
In vitro studies						
Rifampicin-loaded liposomes (RLip) made of soybean phosphatidylcholine; cholesterol and dicetyl phosphate or stearylamine	Thin-film hydration	Expressed in rifampicin concentration (0–25 µM)	Rat alveolar macrophage line NR 8383; human bronchial epithelial and small airway epithelial cells	Respiratory associated cells	RLip showed no marked cytotoxicity, with much higher cell viability than the free rifampicin incubated with the three cell lines over 24 h. There was no inflammatory response observed	Changsan et al. [22]
Soybean lecithin liposomes co-loaded with rifampicin and the complex of isoniazid-phthalocyanine with gamma-cyclodextrin	Heating method, organic solvent-free	0.1–1 mg/mL	HeLa cells and human peripheral lung fibroblasts and epithelial cells	Adenocarcinoma and normal respiratory cells	Following 24–48 h of incubation, no cytotoxicity was observed in the dark. Upon laser irradiation, highly loaded liposomes exhibited dose-dependent cytotoxicity	Nkanga et al. [101]
Paclitaxel-loaded liposomes made of phosphatidylcholine, cholesterol and span 80	Thin-film hydration	0.5–5000 µg/mL	Lung cell line A549	Cancer cells	Liposomes showed no cytotoxicity, while plain drug was cytotoxic following 24–48-h incubation	Utreja et al. [140]
Rifapentine-loaded liposome made of hydrogenated soy phosphatidylcholine, cholesterol and Stearyl amine	Spray drying method	20–100 µg/mL	Lung cell line A549	Cancer cells	The formulation exhibited better cell viability than free drug following 24-h incubation	Patil-Gadhe et al. [108]
Melittin-loaded liposomes containing poloxamer 188	Not reported	Expressed in melittin concentration (2 µM)	HepG2 cells	Hepatic carcinoma cells	Empty liposomes showed no cytotoxicity while the melittin-liposomes were as cytotoxic as free melittin	Mao et al. [89]
Cabazitaxel-liposomes made of egg phosphatidyl lipid-80, PEG-phosphoethanolamine and cholesterol	Thin-film hydration	Expressed in cabazitaxel concentration (10–20 µg/mL)	CT-26 and 4T1 cells	Mouse colon and breast cancer cells	Liposomal cabazitaxel showed lower cytotoxicity than the plain drug solution over 48 h of incubation	Yin et al. [157]
Stearyl triphenylphosphonium liposome (STPP-L) and triphenylphosphonium-PEG-phosphatidylethanolamine liposome (TPP-PEG-L)	Thin-film hydration	0–500 µg/mL	HeLa cells	Adenocarcinoma cells	Following 24-h incubation, TPP-PEG-L showed no cytotoxicity, while STPP-L was toxic (IC_{50} 83 µg/mL), but to lesser extent than STPP + PEG-L (IC_{50} 130 µg/mL)	Biswas et al. [18]

Table 1 (continued)

Formulation composition	Preparation method	Liposome dose (administration route)	Animal/cell type	Cell/tissue target	Biocompatibility-/toxicity-related outcomes	References
Isoniazid-liposomes made of dipalmitoylphosphatidylcholine	Thin-film hydration	0.1–1 mg/mL	L929 cells and human blood	Mouse fibroblast cells and human erythrocytes	No haemolysis was observed. Fibroblast morphology and monolayer confluence were unchanged after 24-h incubation	Chimote and Banerjee [24]
Cationic liposomes containing phosphatidylethanolamine and positively charged cholesterol	Thin-film hydration	5–65 µg/mL	Human kidney 293, liver carcinoma HepG2 and mouse fibroblast NIH3T3 cells	Kidney, liver and embryonic tissues	Liposomes showed much lower toxicity than lipofectin and polyethylenimine at concentrations required for optimal gene transfection	Joon Sig Choi et al. [63]
Lipid-based Mitomycin C prodrug in PEG-coated liposome (hydrogenated soybean phosphatidylcholine and distearoyl phosphatidyl ethanolamine)	Thin-film hydration	Expressed in mitomycin C concentration (200–2000 nM)	Mouse carcinoma M109 cells	Murine lung tissues	In the absence of reducing agents (such as cysteine), liposome was fivefold to sixfold less cytotoxic than free mitomycin. No difference was observed on addition of the reducing agents	Gabizon et al. [40]
Cationic lipids with a quaternary ammonium headgroup (CDA14) and a tripeptide headgroup (CDO14)	Thin-film hydration	15 µg/mL and 120 µg/mL	NCI-H460 cells	Human non-small cell lung cancer tissues	CDA14 induced more apoptosis than CDO14. CDA14 showed increased caspase-3/-9 activity with lower mitochondrial membrane potential and higher reactive oxygen species (ROS) levels	Cui et al. [28]
Doxorubicin (Dox) loaded in liposomes made of distearoyl phosphatidylethanolamine-maleimide and cholesterol	Thin-film hydration	Expressed in doxorubicin concentration 1–10 µg/mL	4T1 cell line	Breast tumour cells	Blank liposomes showed no effects on cells. Dox-loaded liposomes showed much better cytotoxic effects on tumour cells than free doxorubicin, which was due to enhanced cell uptake thanks to maleimide handles	Tang et al. [138]

Table 1 (continued)

Formulation composition	Preparation method	Liposome dose (administration route)	Animal/cell type	Cell/tissue target	Biocompatibility-/toxicity-related outcomes	References
Integrated Nanotherapeutics Inc. proprietary anionic, neutral and cationic lipids	Not disclosed	0–128 µg/mL	HL60, NB4, A549 and NIH3T3 cell lines	Tumour cell lines and healthy fibroblasts	Liposomes loaded with siRNAs did not affect viability both suspended and adherent cells at conventionally used concentrations	Syama et al. [135]
mRNA mixed with positively and negatively charged lipids (DOTAP/POPS)	Thin-film hydration, extrusion, microfluidics	0–48 µg/mL	Neuro-2a cells	Brain tissues	At 0.288 mg/mL positively charged liposomes led to 65% cell apoptosis, while no apoptosis was obvious for negatively charged liposomes; only 0.48 mg/mL caused 50% apoptosis. Mixing cationic with anionic lipids led to 80% cell viability	Wang et al. [144]
In vivo studies						
Paclitaxel-loaded liposomes made of phosphatidylcholine, cholesterol and span 80	Thin-film hydration	10–200 mg/kg (IP)	Swiss albino mice	Liver, kidney, heart and spleen	No mortality, haematological, biochemical, histopathological, or weight changes were observed over 28 days	Utreja et al. [140]
Rifapentine-loaded liposome made of hydrogenated soy phosphatidylcholine, cholesterol and Stearyl amine	Spray drying method	1–10 mg/kg (Intratracheal)	Wistar rats	Lung	No changes in biochemical, histopathological parameters or body weight were observed at 1–5 mg/kg, while 10 mg/kg led to remarkable tissue toxicity and animal death	Patil-Gadhe et al. [108]
Melittin-loaded liposomes containing poloxamer 188	Not reported	2–8 mg/kg (SC)	LM-3 xenograft tumour model	Hepatocellular carcinoma tissue	The liposomal melittin suppressed tumour growth with reduced side effects compared to the plain melittin	Mao et al. [89]
Cabazitaxel-liposomes made of egg phosphatidyl lipid-80, PEG-phosphoethanolamine and cholesterol	Thin-film hydration	5 mg/kg (IV)	Balb/c mice	Erythrocyte, liver, spleen, kidney, heart and tumour tissues	Unlike the plain drug, cabazitaxel liposomes showed no significant haemolysis or histological lesions and stable body weight 48 h post-injection	Yin et al. [157]

Table 1 (continued)

Formulation composition	Preparation method	Liposome dose (administration route)	Animal/cell type	Cell/tissue target	Biocompatibility-/toxicity-related outcomes	References
Doxorubicin-liposomes made of PEG/phosphatidylcholine and cholesterol with Anti-CD19 mAb targeting ligand	Thin-film hydration	10.4–13.6 mg/kg (IV)	SCID mice	Heart and blood	Drug-free liposomes showed no lethal toxicity. Targeted doxorubicin–liposomes increased mice life span to much higher levels than non-targeted ones, which were still better than plain doxorubicin	Allen et al. [4]
Multivalent cationic liposome (Lipofectamine™), monovalent cationic DOTAP liposomes, neutral and negative liposomes	Heating method, organic solvent-free	200 nmol/mouse (intratracheal instillation)	Male Balb/c mice	Lung tissues	Lipofectamine™ induced greater toxic reactive oxygen intermediates than DOTAP liposomes, while neutral and negative liposomes showed no toxicity 24 h post-intratracheal instillation	Dokka et al. [31]
Lipid-based Mitomycin C prodrug in PEG-coated liposomes (hydrogenated soybean phosphatidylcholine and distearoyl phosphatidyl ethanolamine)	Thin-film hydration	10 mg/kg/week (IV)	Female Balb/c mice	–	A single dose (10 mg/kg) of free mitomycin C exhibited drastic weight loss and toxic death, while the liposomes caused fatal toxicity only after three doses, and no weight loss was observed	Gabizon et al. [40]
DOTAP cationic liposomes containing cholesterol	Thin-film hydration	10, 25 or 100 mg/kg/day (IV)	Male Wistar rats	Liver, kidney, lung, brain and spleen	Histological, haematological and chemico-clinical evaluations showed no significant changes after repeated doses. Dose-dependent genotoxicity (DNA strand breaks) was observed in the lung	Knudsen et al. [71]

Table 1 (continued)

Formulation composition	Preparation method	Liposome dose (administration route)	Animal/cell type	Cell/tissue target	Biocompatibility-/toxicity-related outcomes	References
Doxorubicin (Dox) loaded in liposomes made of distearoyl phosphatidylethanolamine-maleimide and cholesterol	Thin-film hydration	Amount equivalent to 5 mg/kg Dox (IV)	BALB/c mice	Heart tissues	The cardiac cavity of animals treated with Dox-loaded liposomes remained unchanged, while free doxorubicin animals exhibited several abnormalities (e.g. loose structure, myocardial vacuole degeneration, scattered inflammatory cell infiltration)	Tang et al. [138]
PEGylated mitoxantrone liposomes from CSPC Zhongqi Pharmaceutical Technology (Shijiazhuang) Co., Ltd.	Not disclosed	20 mg/m^2 (IV)	Randomized, open-label, active-controlled, single centre, phase II clinical trial with Chinese patients with advanced breast cancer	Breast	Liposomes exhibited lower incidence of cardiovascular disorders (13.3% vs. 20.0%) and increased cardiac troponin T (3.3% vs. 36.7%), but higher incidence of anaemia (76.7% vs. 46.7%), skin hyperpigmentation (66.7% vs. 3.3%) and fever (23.3% vs. 10.0%) than free mitoxantrone	Wang et al. [143]
Cholesterol, egg phosphatidylcholine (Egg-PC) and 1,2-distaroyl-sn-glycero-3-phosphoethanolamine-N-[methoxy(polyethylene glycol)$_{2000}$] and drug conjugate cholesterol-SN38	Ethanol injection	15 mg/kg (IV)	ICR mice	Liver, heart, lung, spleen, kidney and ileum	The liposomal formulation of prodrug improved drug tolerability by alleviating bloody diarrhoea and liver damage, which were reported side effects of the prodrug	Shi et al. [126]

on liposome toxicity has also been demonstrated. As an example, through generation of reactive oxygen species, polycationic liposomes (Lipofectamine™) exhibited much higher lung toxicity than monocationic liposomes made of 1,2-dioleoyl-3-trimethylammonium-propane (DOTAP) [32]. In the same study, no toxicity was observed with neutral and negative liposomes made of phosphatidylcholine and a mixture of phosphatidylcholine and phosphatidylglycerol, respectively.

In addition to particle size and charge, the influence of liposome surface chemistry (such as PEGylation and ligand decoration) on the formulation's biocompatibility has been investigated. Biswas et al. observed that stearyl triphenyl-phosphonium PEGylated liposomes showed much better HeLa cells' viability (IC_{50} 130 µg/mL) than the non-PEGylated liposomes counterpart (IC_{50} 83 µg/mL) [19]. A good example of the influence of targeting on liposome biocompatibility is the study by Allen et al. [5], which also illustrates the advantage of a slower release profile over a faster release behaviour on doxorubicin toxicity. The authors observed that doxorubicin-liposomes decorated with anti-CD19 antibodies increased the mice life span to much higher levels than non-targeted doxorubicin-liposomes, though the latter were found to be still better than plain doxorubicin. The improvement in the drug's safety profile through liposomal delivery arises from the fact that liposomes hold a great potential to alter drug biodistribution. Another illustrative example of liposomes improving drug toxicity profile is the work by Kuang et al. [74]: this study demonstrated that anionic long-circulating liposomes significantly reduced the accumulation of cisplatin in murine kidneys, which is an elegant strategy to prevent cisplatin's acute renal toxicity. This is similar to the observation that liposomes suppress the cardiotoxicity of doxorubicin due to reduced accumulation in myocardia tissues [139], which led to successful implementation of marketed doxorubicin liposomal products (i.e. Doxil® and Myocet®).

Liposomes often alter drug circulation in a beneficial way, but liposome accumulation in the RES tissues (liver, spleen, etc.) can be problematic. Therefore, most in vivo studies consider histopathological evaluations of RES organs to assess tissue degeneration or necrosis due to the administered nanoproduct. As shown in Table 1, many authors observed no histopathological changes in the RES tissues of mice following treatment with therapeutic liposomes [71, 140, 157]. Nevertheless, careful safety profiling requires insights beyond histopathological evaluations, looking into molecular biomarker analysis to detect signs of nonnecrotic biological perturbations. In conjunction with this, the work by Knudsen et al. is an appealing illustration, where the biocompatibility of DOTAP cationic liposomes was evaluated [71]. According to the data, the histological, haematological and chemico-clinical evaluations indicated no significant changes after repeated doses, while genotoxicity assessment revealed elevated expression of cytokine genes and DNA strand breaks in the lung and spleen tissues (Fig. 4A). These findings are arguably part of the scarce data demonstrating the need for a thorough organ-function assessment when characterizing the safety profile of emerging NP formulations.

2.2.2.2 PLGA systems The inherent biosafety of PLGA arises from the fact that its biodegradation releases lactic and glycolic acids as by-products, which both enter the Kreb's cycle for safe metabolization into carbon dioxide and water [128]. However, careful biocompatibility profiling entails thorough toxicological consideration including not only polymer intrinsic properties but also relevant biological parameters such as tissue-polymer interactions or tissue exposure to the laden polymeric matrix, which can lead to intolerable inflammatory or immunological responses [117]. In this context, types of PLGA-based constructs (*i.e.* implants, microparticles or NPs) are of paramount importance due to inconsistent in vivo responses observed. For instance, implants can cause prolonged local reactions throughout polymer degradation, while NPs may lead to intracellular disturbances due to high cell penetration and broad biodistribution [86]. The biocompatibility of all the PLGA systems has been recently reviewed [35]. As a biocompatible vehicle, PLGA NPs have demonstrated some potential to control drug product biosafety. For instance, the haemolytic effect of the antibiotic amphotericin B was significantly reduced when used in the form of amphotericin B-loaded PLGA NPs, which was solely attributed to the slow release behaviour of NPs [93]. In another study, PLGA NPs exhibited dose-dependent cytotoxicity, but the overall safety profile was much better than that of dendrimers, since the former showed acceptable cytocompatibility up to 180 µg/mL (despite their larger sizes, 140 nm), while the latter were highly cytotoxic at 2.8 10^{-4} M (though being of smaller sizes, 10 nm) [31].

The impact of surface chemistry on cytocompatibility of PLGA NPs was elucidated by Gossmann et al. [46]. These authors observed that non-decorated PLGA NPs loaded with didodecyldimethylammonium bromide exhibited much higher cytotoxicity on Caco-2 cell line than their PEGylated formulation counterparts (EC_{50} 54.8 vs 996.5 µg/mL, respectively); this was further explained by enhanced NPs dispersion and absence of aggregation due to PEG chains [47]. A similar observation was reported by Cai et al., who noted that PEG-PLGA NPs containing poly-*L*-orithine/fucoidan were less cytotoxic than non-PEGylated NPs of the same composition [22]. Another

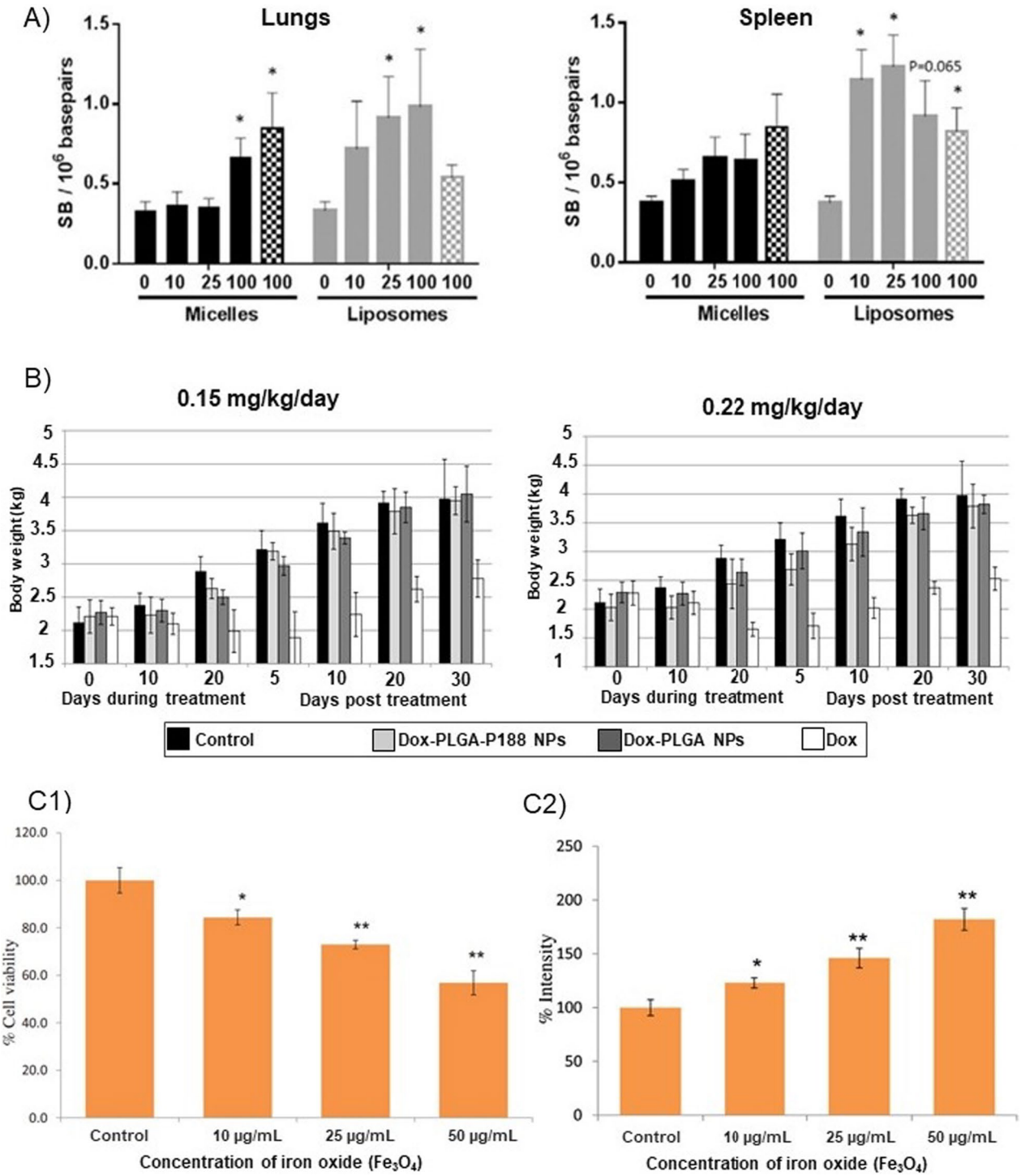

Fig. 4 **A** Level of DNA damage expressed as strand breaks (SB), 24 h (plain bars) and 48 h (dashed bars) following IV injection of nanoparticles (0–100 mg/kg body weight) to Wistar rats ($n=8$)—illustrating increasing DNA damage due to tissue exposure to liposomes (*$p<0.05$ vs control). Reprinted from [71], an article published under the terms of the Creative Commons Attribution-NonCommercial-ShareAlike Licence (CC BY-NC-SA 3.0). **B** Change in Chinchilla rabbits body weight ($n=10$) following daily IV injection of doxorubicin (Dox)-loaded PLGA NPs with and without poloxamer 188 coat (P188)—illustrating the toxicological benefit of Dox encapsulation in NPs. Reprinted from [111], with permission from Elsevier (licence number 5474400895276). IONPs concentration-dependent MTT cytotoxicity (C1) (*$p<0.05$; **$p<0.01$ vs control) and % induction of ROS generation (C2) (*$p<0.01$; **$p<0.001$ vs control) in human lung alveolar epithelial cells following incubation over 24 h ($n=3$)—highlighting oxidative stress as mechanism for IONPs cytotoxicity. Reprinted from [34], with permission from Elsevier (licence number 5474441325417)

variable parameter investigated in PLGA NPs biosafety profiling encompasses the routes of administration. In a comparative toxicological study, amphotericin B laden PLGA NPs administered orally and intraperitoneally demonstrated no nephrotoxicity nor hepatotoxicity in Wistar rats irrespective of the routes, while marketed deoxycholate amphotericin B formulation caused hepatic cellular alteration following administration through the same routes [93]. As illustrated in Table 2, many studies reported various biocompatibility profiles of PLGA NPs depending on the chemical composition and functionalities [51, 92, 125, 132]. Among the important observations from PLGA nanotoxicity studies is the meticulous analyses of biosafety that explored broader toxicological parameters. An illustrative example is the study by He et al. [55, 56]. The authors established the biosafety of monomethoxy-PEG-PLGA-poly(*L*-lysine) NPs by assessing (1) protein synthesis, cell membrane integrity and chromatin agglutination in Huh7, L02 and RAW 264.7 cells; (2) the release of interleukin-1β, tumour necrosis factor-α and transforming growth factor-β1 from THP-1 cell-derived macrophages; and (3) the potential impact on embryonic development using zebrafish embryos. Moreover, nanotoxicity assessment is required to involve chronic toxicity studies in addition to acute toxicity studies to better inform on the biosafety profiles of nanoproducts. For example, acute toxicity studies recently showed no difference between plain doxorubicin versus doxorubicin-loaded PLGA NPs [111]; however, chronic toxicity data demonstrated that the encapsulation of doxorubicin in PLGA NPs significantly improved drug safety profile (Fig. 4B). Rigorous exploration of nanotoxicity being one the utmost requirements for translational development, such extensive safety profiling appears to be highly inspirational for nanotechnologists.

2.2.2.3 Iron oxide nanoparticles SPIONs are associated with nanometric sizes and high surface to volume ratios that promote the biological reactivity of particles (as the case for all NPs in general). However, due to enhanced reactivity and propensity to diffuse through biological barriers, the nanoscale regime of SPIONs is the motor for their interference with the structure and functions of tissues or organs [129]. Therefore, commendable efforts have been dedicated to SPIONs' nanotoxicity assessment to improve the safety profile of each individual product under development. Many reviews have recently discussed the toxicity and biocompatibility of SPIONs [10, 147, 152, 158]; hence, the few data presented in Table 3 solely serve as illustrative references for emerging nanotechnologies.

Apart from the general NP toxicological parameters (related to particle characteristics and pharmacological factors), the intrinsic toxicity of SPIONs are attributed to both the iron core and surface coatings [10]. The toxicity mechanisms inherent in the iron core include the generation of reactive oxygen species (ROS) causing oxidative stress [34], and the iron overload that alters iron homeostasis leading ultimately to cell death (Fig. 4C1, 2). Following endocytosis, iron particles are metabolized in iron ions that further diffuse into the nucleus and mitochondria, where they react with oxygen and hydrogen peroxide through oxidative reduction to generate ROS [9, 155]. Regarding the surface chemistry side, studies have demonstrated the chief influence of coatings on SPIONs' biocompatibility profiles, due to their impact on particle size, surface charge and oxidative site accessibility. For instance, PEGylation has shown great potential to reduce the toxicity of SPIONs both in vitro [106] and in vivo [114]. The positive impact of surface chemistry on SPION toxicity was also observed with non-polymeric coatings, such as curcumin and silica layers that were used by Malvindi et al. [88] and Bhandari et al. [16], respectively. Nevertheless, most coating–toxicity relationships have been established in vitro, hence there is a pending need for further confirmation under in vivo conditions. In fact, an instructive study showed that PEGylated SPIONs that were reported to be nontoxic in vitro were found to cause liver and kidney injury [127], likely because of in vivo xenobiotic metabolization (based on the intracellular toxicity mechanisms explained early). Another important parameter is the SPION surface charge, which is consistent with some of the general nanotoxicity rules, postulating that positively charged particles are toxic while neutral and negatively charged particles are expected to be safe. Cationic coatings like polyethylenimine (PEI) have shown the potential to yield toxic SPIONs, while neutral or poorly charged PEGylated particles were found to be safer under the same conditions [38, 58].

While many studies have demonstrated the possibility of tuning the characteristics of SPIONs for enhancing biocompatibility by means of cell viability or proliferation assays, some authors have investigated subcellular and molecular perturbations for a diligent biosafety profiling. As an example, Pongrac et al. evaluated the potential toxicity of SPIONs with different coatings (*D*-mannose or poly-*L*-lysine) using murine neural stem cells as a regenerative medicine model [112]. Data showed that both uncoated and coated SPIONs (regardless of the coating) exhibited adverse effects at subcellular levels (e.g. loss of mitochondrial homeostasis, DNA damage, etc.), while cell viability remained unchanged after 24 h of incubation with up to 200 µg/mL. Such studies evidence the need for careful characterization of nanotoxicity to engineer NPs with a good safety profile. Despite their clinical relevance, SPIONs under development exhibit inherent toxicity

Table 2 Summary of representative studies evaluating the biocompatibility and toxicity of some PLGA-based NPs

Formulation composition	Preparation method	Dose (administration route)	Animal/cell type	Cell/tissue target	Biocompatibility-/toxicity-related outcomes	References
In vitro studies						
Fluorescein amine-labelled PLGA mixed with ε-caprolactone–PEG copolymers	Nanoprecipitation technique–solvent evaporation	18–180 µg/mL	L929 cell line	Mouse fibroblasts	PLGA-based NPs exhibited no changes in fibroblasts morphology and confluent monolayer after 48-h incubation, while dendrimers led to altered morphology and detachment in a dose-dependent way	Do et al. [30]
Gold NPs-coated polydopamine-modified PLGA capsule hybrid	Double emulsion, solvent evaporation	10–1000 µg/mL	ECA-109 cell line	Human oesophageal cancer cell	No remarkable cytotoxicity: cell viability was same as the control cells treated with PBS over 24 h	Xi et al. [149]
Monomethoxy-PEG-PLGA-poly(*L*-lysine) NPs	One-step oil-in-water emulsion, solvent evaporation	10–1000 µM	RAW 264.7, Huh7 and L02 cells	Murine macrophage, human hepatic carcinoma and normal embryo liver cells	No effect on cell membrane integrity, protein synthesis and chromatin stability, except dose-dependent and time-dependent increase in the content of reactive oxygen species. No significant induction of inflammatory cytokines	He et al. [55]
folic-acid-grafted-PEG-PLGA NPs co-loaded with cisplatin and paclitaxel	One-step oil-in-water emulsion, solvent evaporation	0.01–1 mg/mL	New Zealand white rabbits' blood; M109 and A549 cells	Rabbit erythrocyte, murine and human lung carcinoma cell	Drug-free NPs exhibited no overt cytotoxicity, haemolysis, blood clotting or complement activation	He et al. [53]
Amphotericin B-loaded PLGA NPs decorated with dimercaptosuccinic acid ligand	Water-in-oil emulsification, solvent evaporation	1.56–600 µg/mL	Human blood and peritoneal tissues	Erythrocyte and peritoneal macrophages	Drug-loaded NPs were less haemolytic than plain drug. NPs showed no cytotoxicity, while free drug was toxic	Souza et al. [130]
Biotin/lactobionic acid-modified PEG-PLGA-PEG NPs co-loaded with curcumin and 5-fluorouracil	Nanoprecipitation technique–solvent evaporation	50–800 µg/mL	Hep G2 and HL 7702 cells	Human hepatocytes and hepatoma cells	Unlike drug-loaded NPs, the blank NPs showed no overt cytotoxicity after 48 h of incubation	Ni et al. [97]

Table 2 (continued)

Formulation composition	Preparation method	Dose (administration route)	Animal/cell type	Cell/tissue target	Biocompatibility-/toxicity-related outcomes	References
Didodecyldimethylammonium bromide (DMAB)-stabilized PLGA modified with polyvinyl alcohol (PVA) or PEG	One-step oil-in-water emulsion, solvent evaporation	0.5–1000 µg/mL	Caco-2 cell line	Human epithelial colorectal adenocarcinoma cells	DMAB-PLGA NPs modified with PVA or PEG showed no cytotoxicity, while unmodified NPs induced significant concentration-dependent necrosis, apoptosis and chromatin disturbance	Gossmann et al. [46]
PLGA-poly(3-hydroxybutyrate) nanocomposite extract	Needle-punching nonwoven fabric synthesis catalysed by $Zr(AcAc)_4$	Not indicated	Fibroblast-like cell line L929	Mouse fibroblast	No cytotoxic or genotoxic effects were observed following 72 h of incubation	Krucinska et al. [73]
PLGA NPs loaded with TRITC-in-polyethyleneimine	Double emulsion, solvent evaporation	Not indicated	Male and female gametes	Sperms, oocytes	No distinct morphological, chromosomal abnormalities, transgenerational effects or genetic aberrations were observed	Kim et al. [70]
PLGA-(poly-*L*-orithine/fucoidan) core–shell NPs	One-step oil-in-water emulsion, solvent evaporation	5–100 µg/mL	MCF-10A cell line	Breast epithelium cells and rabbit blood cells	Cell morphology was unchanged, but proliferation pattern was affected in a time-dependent way. Haemolysis rates increased with NPs concentrations	Cai et al. [21]
PLGA NPs	Nanoprecipitation, solvent evaporation	0.1–0.4 mg/ml	Primary human myoblasts and myotubes	Skeletal tissues	PLGA NPs did not decrease cell viability, while liposomes and silica NPs showed concentration-dependent and time-dependent decrease in cell viability	Guglielmi et al. [49]
PEG-PLGA, PEG-poly(*L*-lactide) (PLA) and PEG-PLA-PEG NPs	One-step oil-in-water emulsion, solvent evaporation	0.05–1 mg/ml	Fibroblast-like cell line L-929 and human umbilical vein endothelial cell	Mouse fibroblasts, blood, human macrophages and human vascular endothelium	No significant cytotoxicity observed. Adverse effects of PEG-PLGA NPs on haemolysis and inflammatory cytokines release were the highest while PEG-PLA-PEG NPs' were the lowest	Shen et al. [125]

Table 2 (continued)

Formulation composition	Preparation method	Dose (administration route)	Animal/cell type	Cell/tissue target	Biocompatibility-/toxicity-related outcomes	References
PLGA NPs loaded with Chondroitinase ABC (ChABC)	Double emulsion, solvent evaporation	1500–6000 µg/mL	Olfactory ensheathing cells	Rat olfactory mucosa	Following 48 h of incubation, there were no significant differences between the control and NP-treated cell viability	Azizi et al. [11]
Chitosan-coated PLGA nanoparticles loaded with bevacizumab	One-step oil-in-water emulsion, solvent evaporation	Not reported	Fertilized fresh hen's eggs	Hen's egg chorioallantoic membrane	NPs formulation was non-irritant and tolerated to chorioallantoic membrane after	Pandit et al. [104]
Cell-penetrating peptides decorating DNA-loaded PLGA nanoparticles	Double emulsion-solvent evaporation method	0.075–1.2 mg/mL	A549 and Beas-2B cells	Lung tissues	After 24-h incubation of NPs with cells, there was no change in mitochondrial activity and membrane integrity In addition, the inflammatory response and levels of apoptosis were significantly lower, and there was no activation of caspase-3	Dos Reis et al. [32]
In vivo studies						
Monomethoxy-PEG-PLGA-poly(*L*-lysine) NPs	One-step oil-in-water emulsion, solvent evaporation	10–1000 µM	Zebrafish embryos	Heart	No effect on embryonic heartbeat rate, malformation or survival. At extreme concentrations (> 500 µM), NPs induced reactive oxygen species production at early stage of embryonic development	He et al. [54]
PLGA-poly(3-hydroxybutyrate) nanocomposite bone implant	Needle-punching nonwoven fabric synthesis catalysed by $Zr(AcAc)_4$	Surgical femur implantation	New Zealand breed male and female rabbits	Blood, RES organs, stomach, small and large intestine, testes, uterus, heart	The blood cells remained unchanged. No significant differences between enzymes values from the test and control groups following 180 days of implantation	Krucinska et al. [73]

Table 2 (continued)

Formulation composition	Preparation method	Dose (administration route)	Animal/cell type	Cell/tissue target	Biocompatibility-/toxicity-related outcomes	References
Biotin/lactobionic acid-modified PEG-PLGA-PEG NP	Nanoprecipitation, solvent evaporation	200 mg/kg every 2 h (IV)	Female nude balb/c mice	Liver, spleen, kidneys, lunges and heart	No obvious signs of cellular or organ injury or inflammation were observed, and no death was recorded after injection of up to 2000 mg/kg in total	Ni et al. [97]
PLGA NPs loaded with TRITC-in-polyethyleneimine	Double emulsion-solvent evaporation method	Not indicated	ICR mice	Murine embryos	No influence on embryo development to the blastocyst	Kim et al. [70]
Amphotericin B-loaded PLGA and PLGA-PEG blend NPs	One-step oil-in-water emulsion, solvent evaporation	10 mg/kg/day (oral or IP)	Male Wistar rat	Liver, kidneys and blood cells	Biochemical and histopathological parameters remained unchanged after 7 days of treatment. Unlike the plain drug, NPs showed no blood cell damage	Moraes Moreira Carraro et al. [93]
Amphotericin B-loaded PLGA NPs decorated with dimercaptosuccinic acid ligand	Water-in-oil emulsification, solvent evaporation	6 or 30 mg/kg/day (IP)	Healthy balb/c or Swiss mice	Blood, peritoneal, bone marrow cells	No significant difference between the DNA from mice treated with NPs and PBS, while control (cyclophosphamide) caused DNA damage. NPs showed similar neutrophils, leucocytes and monocytes as PBS, unlike the plain drug	Souza et al. [130]
PLGA-(poly-L-orithine/fucoidan) core–shell NPs	One-step oil-in-water emulsion, solvent evaporation	300 mg/kg (IP)	SPF mice	Liver and kidney	NPs showed no significant differences with negative control in body weight and histological parameters. No death or apparent toxicity was observed	Cai et al. [21]
PEG-PLGA, PEG-poly(L-lactide) (PLA) and PEG-PLA-PEG NPs	One-step oil-in-water emulsion, solvent evaporation	0.05–1 mg/ml	Zebrafish embryos	Heart and yolk sac	The concentration-dependent adverse effects of PEG-PLGA NPs on embryo survival and growth were the highest, while PEG-PLA-PEGs were lowest	Shen et al. [125]

Table 2 (continued)

Formulation composition	Preparation method	Dose (administration route)	Animal/cell type	Cell/tissue target	Biocompatibility-/toxicity-related outcomes	References
PLGA NPs and surface-modified PLGA chitosan NPs	One-step oil-in-water emulsion, solvent evaporation	12 mg/kg/day (oral)	F344 rats	Spleen, kidney, liver, lung, brain, intestine, heart	No significant histological changes seen in tested organs, except for intestine and liver. Body weight remained unchanged	Navarro et al. [96]
Doxorubicin-loaded PLGA nanoparticles coated with poloxamer 188	Double emulsion-solvent evaporation technique	0.15–0.22 mg/kg/day (IV)	Chinchilla rabbits	Blood, Spleen, kidney, liver, lung, brain, intestine, heart	PLGA NPs significantly lowered the haematological, cardiac and testicular toxicity of the drug, but dose-dependent functional and morphological abnormalities were observed	Pereverzeva et al. [111]
Cx43MP peptide loaded PLGA nanoparticles	Nanoprecipitation technique–solvent evaporation	10–500 µg/mL	Zebrafish embryo toxicity (ZET) model	Embryos	Zebrafish remained normal 144 h after fertilization with the NPs; no significant malformations or cytotoxicity were obvious	Bisht and Rupenthal [17]
PLGA nanoparticles	Sonication method	100 µg/ml	BALB/c mice	Mouse cortical neuronal tissue	PLGA nanoparticles greatly protected neuronal cells against the aggregation of amyloid β (Aβ) peptide and showed favourable impact on the expression of AD-related genes/proteins	Wu et al. [148]
PLGA and PEG-PLGA nanoparticles	Sonication, solvent evaporation	1–25 µM	BALB/c mice	Frontal cortex from pup brains	PLGA nanoparticles inhibited β-amyloid (Aβ) peptides aggregation and triggered the disassembly of their aggregates beyond physiological temperatures, protecting neurons against Aβ-mediated toxicity	Paul et al. [109]

Table 3 Summary of representative studies evaluating the biocompatibility and toxicity of SPIONs

Formulation composition	Preparation method	Dose (administration route)	Animal/cell type	Cell/tissue target	Biocompatibility-/toxicity-related outcomes	References
In vitro studies						
SPIONs decorated with hyaluronic acid and transferrin	Chemical coprecipitation	25–250 µg/mL	HeLa cells	Adenocarcinoma cells	No significant difference in cell viability between SPIONs and PBS control following 24-h incubation	Pan et al. [103]
SPIONs capped with PEG or triethylene glycol	One-pot decomposition of iron(III) acetylacetonate in triethylene glycol	1–160 µg/mL	Mouse fibroblast cells	Normal mouse fibroblasts	Except some morphological changes, all the SPIONs showed no significant decrease in cell viability when compared to the controls after 72-h incubation	Arteaga-Cardona et al. [10]
SPIONs coated with sodium oleate (SO-IONPs), or with SO + PEG (SO-PEG-IONPs), or with SO + PEG + PLGA (SO-PEG-PLGA-IONPs)	Chemical coprecipitation	0.1–100 µM	Mouse L5178Y lymphoma and Bhas 42 cells	Cancerous cells	SO-IONPs and SO-PEG-PLGA-IONPs showed no mutagenicity, while the effect of SO-PEG-IONPs was ambiguous. SO-PEG-PLGA-IONPs were carcinogenic in a concentration-dependent manner	Gábelová et al. [39]
SPIONs solubilized with PEG	Chemical coprecipitation	1–150 µM	MCF-7 cells	Breast cancer cell	No remarkable decrease in cell viability or change in cell cycle progression after 24-h incubation	Kansara et al. [67]
SPIONs solubilized with tetramethylammonium11-aminoundecanoate	One-pot decomposition of iron(III) acetylacetonate in 1,2-hexadecanediol	0.1–100 µg/mL	G9T, SF126, U87, MB157, SKBR3, WI-38, SVGp12	Human normal, glia and breast cancer cells	No cytotoxicity up to 10 µg/m, but overt decrease in cell viability at 100 µg/mL following 72 h of incubation	Ankamwar et al. [6]
Core–shell Fe_3O_4–Au composite magnetic NPs	Chemical coprecipitation	25–100 mg/mL	Mouse fibroblast cell line (L-929)	Murine fibroblasts	No significant difference in cell viability between the experimental group and the control following 48-h incubation	Li et al. [82]
Ag-, Au-, Cs- or Pt-coated Fe_3O_4 microparticles	Chemical coprecipitation	2.5–40 mg/mL	Mouse fibrosarcoma cell line (L-929)	Murine fibroblasts	Naked particles showed no cytotoxicity below 5 mg/mL, while modified ones were not cytotoxic up to 20 mg/mL after 24 h of incubation	Xia et al. [150]

Table 3 (continued)

Formulation composition	Preparation method	Dose (administration route)	Animal/cell type	Cell/tissue target	Biocompatibility-/toxicity-related outcomes	References
Fe_3O_4 nanocrystals coated with PEGylated phospholipid	Thermal decomposition of iron pentacarbonyl	0.003–0.2 mg Fe/mL	HeLa cells	Adenocarcinoma cells	NPs exhibited dose-dependent changes in cell viabilities	Gu et al. [48]
SiO_2-coated SPIONs modified with DMSA	Chemical coprecipitation	1–3 mg/mL	Human blood and Wuzhishan mini-pigs blood	Blood cells	No remarkable coagulation-fibrinolysis or haemolysis over 120 min of exposure	Xiang et al. [151]
Polyethylenimine (PEI)-coated SPIONs modified with PEG	Chemical coprecipitation	6.25–100 µg/mL	SH-SY5Y, U937 and MCF-7 cell lines	Human neuroblastoma, lymphoma and breast cancer cells	Non-PEGylated PEI-particles increased cytotoxicity and ROS production due to high surface charge. Both PEGylated and non-PEGylated cationic IONPs caused cell morphology changes	Hoskins et al. [57]
Polyethylenimine (PEI)-coated and PEG-coated SPIONs	Not reported	3.125–100 µg/mL	RAW264.7 and SKOV-3 cells	Macrophages and ovarian cancer cells	PEI-coated SPIONs caused higher ROS generation, apoptosis than PEG-SPIONs	Feng et al. [37]
Rod and spherical Fe_3O_4 NPs versus Fe_3O_4 microparticles	Not reported	10–200 µg/mL	RAW 264.7 cells	Mouse macrophage	Rod SPIONs showed higher cytotoxicity due to greater membrane damage and ROS production than other particles	Lee et al. [77]
SPIONs decorated with tetraethyl orthosilicate (TEOS), (3-aminopropyl) trimethoxysilane (APTMS), TEOS-APTMS or citrate	Chemical coprecipitation	100–1000 ppm	Mouse fibroblast cell line (L-929)	Murine fibroblasts	SPIONs at higher doses showed variable cytotoxicity and genotoxicity profiles depending on functional groups and particle sizes, while lower doses (below 500 ppm) were safe for all NPs batches	Hong et al. [56]
In vivo studies						
SPIONs decorated with hyaluronic acid and transferrin	Chemical coprecipitation	24 mg Fe/kg (IV)	Female Balb/c nude mice	Blood, heart, liver, spleen, lung and kidney	No obvious changes in organ functional biomarkers investigated. Body weights were maintained over time 30 days	Pan et al. [103]

Table 3 (continued)

Formulation composition	Preparation method	Dose (administration route)	Animal/cell type	Cell/tissue target	Biocompatibility-/toxicity-related outcomes	References
SPIONs capped with PEG or triethylene glycol	One-pot decomposition of iron (III) acetylacetonate in triethylene glycol	50 mg of Fe per mouse (IV)	New Zealand rabbit	Brain, meninges, liver, kidneys, intestines, lungs and spleen	Histopathological analyses revealed no overt structural changes or tissue damage, despite the hepatic and splenic accumulation over 3 days	Arteaga-Cardona et al. [10]
Doxorubicin-loaded SPIONs decorated with folic acid	Chemical coprecipitation	70.75–1132 µg/mL (IV)	Zebrafish embryo and larvae	Heart, nervous system	Unlike plain drug, SPIONs showed no larvae death and morphological changes. Drug cardiotoxicity was overtly reduced	Igartúa et al. [60]
Core–shell Fe_3O_4–Au composite magnetic NPs	Chemical coprecipitation	1.77–19.89 g/kg (IP)	KunMing albino mice, New Zealand rabbits and beagle dog	Murine blood, heart, spleen, lung, kidney and brain	No obvious histopathological changes (after 2 weeks) or haemolysis. No increase in micronucleus formation. Dogs liver injection (0.1 g/kg) exhibited no acute tissue toxicity after 4 weeks)	Li et al. [82]
Ag-, Au-, Cs- or Pt-coated Fe_3O_4 microparticles	Chemical coprecipitation	5000 mg/kg (oral)	Spleen-deficient rats	Blood cells, bone marrow, liver	Cs-coated and naked Fe_3O_4 particles showed DNA/chromosome damage and haemolysis. Au, Ag and Pt coating improved biosafety profile of Fe_3O_4	Xia et al. [150]
Dextran-coated SPIONs decorated with goat anti-mouse IgG and Fe_3O_4 polystyrene-coated microparticles	Not reported	1.65–1.69 mg/eye (intravitreal injection)	Sprague–Dawley rats	Eye	Injected and noninjected eyes showed no significant differences in intraocular pressure, corneal endothelial cell count, retinal morphology and photoreceptor function over 5 months after injection	Raju et al. [116]

Table 3 (continued)

Formulation composition	Preparation method	Dose (administration route)	Animal/cell type	Cell/tissue target	Biocompatibility-/toxicity-related outcomes	References
Fe_3O_4 nanocrystals coated with PEGylated phospholipid	Thermal decomposition of iron pentacarbonyl	5 mg Fe/kg (IV)	Wild-type BALB/c mice	Liver, spleen and blood	No histopathological or biochemical changes, except an increase in hepatic aspartate transaminase and alanine transaminase. No change in blood counts and body weights over 1 month	Gu et al. [48]
SiO_2-coated SPIONs modified with DMSA	Chemical coprecipitation	0.5–1.0 mg/kg (IV)	New Zealand rabbits and Wuzhishan mini pigs	Liver, kidney, heart, blood	No histopathological, inflammatory or immunostimulatory perturbations over 12 days	Xiang et al. [151]
SPIONs	Not reported	10–200 µg/mL (0.3 mL/egg)	White leghorn (*Gallus gallus domesticus*)	Fertilized eggs	100% mortality at 200 µg/mL. At lower doses (< 100 µg/mL), neuronal loss and body weight decrease were observed after 17–19 days of incubation	Patel et al. [107]
Polyethylenimine (PEI)-coated SPIONs and PEG-coated SPIONs	Not reported	1–5 mg/kg	SKOV-3 tumour-bearing nude mice and BALB/c mice	Spleen, liver, blood	PEI-coated SPIONs showed marked dose-dependent lethal toxicity, while PEG-SPIONs caused no death but rather acceptable tissue toxicity up to 5 mg/kg	Feng et al. [37]

that requires meticulous toxicological testing. The fact that such intrinsically toxic materials have made it to the clinic lends hope for futuristic developments of safer nanoproducts.

2.3 Discussion about NPs characteristics affecting product toxicity

2.3.1 Impact of liposomes characteristics on product toxicity

The characteristics of liposomes, such as size, surface charge and composition, are crucial in determining their toxicity and safety. Smaller liposomes can target tissues more effectively due to enhanced permeability and retention, but may also present higher toxicity levels. For example, smaller liposomes have shown faster drug release and greater toxicity compared to larger counterparts like Doxil liposomes [13]. Strategies such as charge neutralization and PEGylation have been employed to mitigate toxicity and enhance safety. The lipid composition must be carefully balanced to maintain efficacy while minimizing adverse effects. In vitro drug leakage tests are vital for assessing the stability of the lipid bilayer and the encapsulated drug, ensuring controlled drug release under physiological conditions. This is essential for consistent drug delivery to the diseased tissues, which could influence toxicity. As far as drug retention and release are concerned, the internal environment of the liposome, including its volume and ionic concentrations, is critical for drug loading and stability, impacting the toxicity profile [13].

The pharmacokinetics and biodistribution of liposomes are influenced by their size, affecting therapeutic efficacy and toxicity. Smaller liposomes are designed to encapsulate drugs effectively and have extended circulation times, allowing for efficient targeting of specific sites, such as tumour tissues. This targeted delivery is crucial for minimizing exposure to healthy tissues and reducing systemic toxicity. Liposomal drug delivery systems, particularly those modified to reduce cardiotoxicity, optimize the delivery of anticancer drugs, reducing their toxicity [137]. PEGylated liposomes, or 'stealth' liposomes, are designed to evade the immune system and prolong circulation time. PEGylation helps these liposomes avoid clearance by the mononuclear phagocyte system, enhancing drug delivery to tumour sites and reducing toxicity. The pharmacokinetic profile of doxorubicin-loaded PEGylated liposomes differs significantly from doxorubicin alone, due to their size and stealth properties, which allow for targeted and sustained drug release, potentially reducing toxicity to non-target tissues [137].

The surface charge of liposomes affects their tissue distribution, cellular uptake and clearance. Positively charged lipids are linked with higher toxicity, which can be reduced by incorporating negatively charged phospholipids. The ratio of cationic to anionic lipids is pivotal for achieving a balance between safety and efficacy. For instance, it was found that a molar ratio of cationic lipid (DOTAP) to anionic lipid (POPS) of 7:3 achieved the best safety-efficacy balance [144]. The review by Inglut et al. deeply discussed the surface characteristics affecting liposomes toxicity to healthy tissues and unfavourable immune responses [62]. The formulation composition is also critical because it dictates the structural organization of liposomes (such as the morphology and lamellarity), ultimately influencing product safety. The morphology and lamellarity of liposomes affect drug loading and release, which can influence toxicity, as it was previously reported that changes in the particle shape of Doxil liposomes led to complement activation [136]. In summary, the use of liposomes in drug delivery systems requires a thorough understanding of their characteristics to ensure safety and efficacy. Analytical methods and careful experimentation are necessary to elucidate the mechanisms of liposome toxicity, facilitating their safe application in medical treatments [1].

2.3.2 Impact of PLGA nanoparticles characteristics on product toxicity

PLGA is widely researched for drug delivery applications due to its biodegradable nature. Its degradation products are metabolized via the Krebs cycle and are safely cleared by the body. Numerous studies have confirmed PLGA's biocompatibility across various biological tissues, underscoring its suitability for medical use. However, the safety profile of PLGA formulations can be unpredictable due to discrepancies in formulation technologies. These discrepancies arise from the diversity in particulate formulation characteristics and composition, highlighting the necessity for comprehensive nanotoxicity studies to balance risk and benefit trade-offs. The safety and toxicity of PLGA nanoparticles are influenced by several factors, including size, surface charge, biodegradability, concentration and stability. Smaller nanoparticles, with their larger surface area-to-volume ratio, exhibit higher reactivity, which may lead to increased toxicity. This is supported by studies such as [80], which demonstrate that smaller PLGA nanoparticles can significantly trigger the release of TNF-α. However, these nanoparticles did not show notable cytotoxicity at concentrations up to 300 μg/mL [153]. Furthermore, the propensity of nanoparticles to adsorb proteins is a critical consideration, because it influences their in vitro cytotoxicity. Smaller particles, for instance, tend to adsorb more biomolecules, potentially contributing to their cytotoxic effects [153].

The surface charge of PLGA nanoparticles also plays a crucial role in determining their safety profile. For

example, negatively charged PLGA nanoparticles were found to induce a higher inflammatory response in cells [94]. However, a study by Dailey et al. [30] found that PLGA nanoparticles, despite their small size and large surface area, elicited the lowest inflammatory responses compared to non-biodegradable polystyrene nanoparticles. This finding supports the Generally Recognized As Safe (GRAS) status of PLGA's polymeric body. However, surface modifications, such as coatings, can introduce toxicity to PLGA nanoparticles. For instance, Grabowski et al. [48] observed that cytotoxicity and inflammatory responses in A549 human lung epithelial cells varied with surface modification. Solutions containing chitosan, for example, induced similar toxicity levels as corresponding PLGA/chitosan nanoparticle suspensions. Such modifications can alter the surface charge of PLGA nanoparticles, affect their stability in various environments and lead to size variations, ultimately impacting their safety profile [94]. Overall, the safety and efficacy of PLGA nanoparticles are multifaceted, contingent on their size, surface charge, biodegradability and concentration. These factors collectively influence the nanoparticles' interaction with biological systems, their biodistribution and their potential to cause inflammatory responses or other toxic effects.

2.3.3 Impact of SPIONs characteristics on product toxicity

Surface modification techniques, notably PEGylation, are pivotal in mitigating the toxicity of nanoparticles. This strategic alteration aids in circumventing the reticuloendothelial system, thereby significantly reducing toxicity. Such modifications render nanoparticles, particularly SPIONs, more apt for diagnostic and therapeutic applications. Notably, PEGylated SPIONs demonstrate enhanced stability and a marked reduction in undesirable interactions with plasma proteins, a critical factor for ensuring safety in medical applications [78, 114]. In a study by Park et al., different types and concentrations of coatings on SPIONs were found to have varying morphological effects on cells: citric acid-coated SPIONs at high concentrations led to the formation of cytoplasmic vesicles and eventual cell death, while PEGylated SPIONs showed less cytotoxicity [106].

The particle size of SPIONs is a significant determinant in their interaction with biological systems. Smaller particles, due to their distinct biodistribution and toxicokinetics, behave differently compared to their larger counterparts. Particles under 10 nm are typically excreted through renal clearance, while those exceeding 200 nm are predominantly sequestered by the spleen. The ideal size range for medical administration is established between 10 and 100 nm. This size-dependent behaviour, particularly the enhanced cellular penetration of smaller nanoparticles, potentially leads to varied biological effects, as detailed in [87]. Furthermore, the internalization and degradation rates of SPIONs within cells are crucial to their safety. For instance, SiO_2-coated SPIONs have been observed in MRI scans within stem cells for durations of 8–12 weeks, likely attributable to the stability of SiO2 in cellular environments [78].

SPIONs are known to induce oxidative stress, DNA damage and caspase activation, all of which are vital considerations in evaluating their safety. The generation of reactive oxygen species, a key player in SPION-induced genotoxicity, can lead to extensive cellular damage and apoptosis, underscoring the critical role of oxidative stress in nanoparticle-induced toxicity [114].

Biocompatibility emerges as a paramount factor in determining the safety profile of nanoparticles. SPIONs that exhibit biocompatibility show reduced toxicity in vivo, although comprehensive toxicity profiling is essential for their clinical application. Additionally, the impact of nanoparticles on immune cells, such as T-lymphocytes, warrants careful consideration, as discussed in Prabhu et al.'s study [114]. This summarized overview underscores the intricate relationship between the characteristics of SPIONs and their biological interactions. It highlights the necessity for thorough research and meticulous design to ensure the safety and effectiveness of SPIONs in biomedical applications.

3 Conclusions

Successful implementation of nanomedicines in the clinic has motivated continuous investigations to develop high value nanoparticles (NPs) for medical applications. The ability of NPs to operate on the same size scale as biological structures (i.e. nanoscale) is one of the most intriguing features underlying the effectiveness of NPs in medicine. However, sufficient evidence demonstrated that the nanoparticulate nature also sets the ground for potential toxicity, which is likely one of the key challenges affecting their translational development from bench to bedside. In this review, toxicological data from selected clinically approved nanoplatforms (liposomes, PLGA and IONPs) were briefly outlined. This may serve as a practical illustration of the lack of design rules for safe and quality design in nanoengineering since, even for such clinically established nano-systems, there are still limited insights into the direct correlation between the properties of particles and nanotoxicological profiles. The effectiveness and safety of nano-formulations are intricately influenced by factors such as particle size, surface charge, chemical composition, surface coating, solubility and aggregation state. These characteristics play a pivotal role in shaping the interactions of

NPs with biological systems, thereby determining the overall efficacy and safety of the nano-formulations. Although most studies reported no obvious histopathological, apoptotic or necrotic changes caused by NPs, the analysis of the summarized data indicates the lack of organ-function studies as well as the difficulty to compare nanotoxicity data from different protocols, given the discrepancies in doses, models, etc., that make comparison beyond standards. Therefore, unified nanotoxicity assays are highly desired to encourage systematic elucidation of particulate/molecular mechanisms of nanotoxicity and allow the clinical translation of nanomedicines to fully unfold.

Abbreviations

Ag	Silver
APTMS	(3-Aminopropyl) trimethoxysilane
ChABC	Chondroitinase ABC
DMAB	Didodecyldimethylammonium bromide
DOTAP	1,2-Dioleoyl-3-trimethylammonium-propane
Dox	Doxorubicin
IONPs	Iron oxide nanoparticles
GA	Glycolic acid
LA	Lactic acid
MRI	Magnetic resonance imaging
MTT	3-[4,5-Dimethylthiazol-2-yl]-2,5 diphenyl tetrazolium bromide
NPs	Nanoparticles
PEI	Polyethylenimine
PLA	Poly(*L*-lactide)
PLGA	Poly(lactide-*co*-glycolide)
PEG	Polyethylene glycol
PVA	Polyvinyl alcohol
RES	Reticuloendothelial system
RLip	Rifampicin-loaded liposomes
ROS	Reactive oxygen species
SARS-CoV-2	Severe acute respiratory syndrome coronavirus 2
SEM	Scanning electron microscopy
SPIONs	Superparamagnetic nanoparticles
STPP-L	Stearyl triphenylphosphonium liposome
TEM	Transmission electron microscopy
TEOS	Tetraethyl orthosilicate
TPP-PEG-L	Triphenylphosphonium-PEG-phosphatidylethanolamine liposome

Acknowledgements
Thank you to the NGO Förderverein Uni Kinshasa e. V.–BEBUC/Else-Kroener-Fresenius Stiftung & Holger-Poehlmann foundation for their advice.

Author contributions
Not applicable.

Funding
This document has been produced with the financial assistance of the European Union (Grant no. DCI-PANAF/2020/420-028), through the African Research Initiative for Scientific Excellence (ARISE), pilot programme. ARISE is implemented by the African Academy of Sciences with support from the European Commission and the African Union Commission. The contents of this document are the sole responsibility of the author(s) and can under no circumstances be regarded as reflecting the position of the European Union, the African Academy of Sciences and the African Union Commission.

Availability of data and materials
Not applicable.

Declarations

Ethics approval and consent to participate
Not applicable.

Consent for publication
Not applicable.

Competing interests
The author declares that he has no conflict of interest.

Received: 11 February 2023 Accepted: 11 December 2023
Published online: 16 December 2023

References

1. Aillon KL, Xie Y, El-Gendy N, Berkland CJ (2009) Effects of nanomaterial physicochemical properties on in vivo toxicity. Adv Drug Deliv Rev 61:457–466. https://doi.org/10.1016/j.addr.2009.03.010.Effects
2. Aggarwal P, Hall JB, McLeland CB et al (2009) Nanoparticle interaction with plasma proteins as it relates to particle biodistribution, biocompatibility and therapeutic efficacy. Adv Drug Deliv Rev 61:428–437. https://doi.org/10.1016/j.addr.2009.03.009
3. Aisida SO, Akpa PA, Ahmad I et al (2020) Bio-inspired encapsulation and functionalization of iron oxide nanoparticles for biomedical applications. Eur Polym J 122:109371. https://doi.org/10.1016/j.eurpolymj.2019.109371
4. Ali A, Zafar H, Zia M et al (2016) Synthesis, characterization, applications, and challenges of iron oxide nanoparticles. Nanotechnol Sci Appl 9:49–67. https://doi.org/10.2147/NSA.S99986
5. Allen TM, Mumbengegwi DR, Charrois GJR (2005) Anti-CD19-targeted liposomal doxorubicin improves the therapeutic efficacy in murine B-cell lymphoma and ameliorates the toxicity of liposomes with varying drug release rates. Clin Cancer Res 11:3567–3573. https://doi.org/10.1158/1078-0432.CCR-04-2517
6. Almeida JPM, Chen AL, Foster A, Drezek R (2011) In vivo biodistribution of nanoparticles. Nanomedicine 6:815–835. https://doi.org/10.2217/nnm.11.79
7. Ankamwar B, Lai TC, Huang JH et al (2010) Biocompatibility of Fe_3O_4 nanoparticles evaluated by in vitro cytotoxicity assays using normal, glia and breast cancer cells. Nanotechnology. https://doi.org/10.1088/0957-4484/21/7/075102
8. Anselmo AC, Mitragotri S (2019) Nanoparticles in the clinic: an update. Bioeng Transl Med 4:1–16. https://doi.org/10.1002/btm2.10143
9. Apopa PL, Qian Y, Shao R et al (2009) Iron oxide nanoparticles induce human microvascular endothelial cell permeability through reactive oxygen species production and microtubule remodeling. Part Fibre Toxicol 6:1–14. https://doi.org/10.1186/1743-8977-6-1
10. Arias LS, Pessan JP, Vieira APM et al (2018) Iron oxide nanoparticles for biomedical applications: a perspective on synthesis, drugs, antimicrobial activity, and toxicity. Antibiotics. https://doi.org/10.3390/antibiotics7020046
11. Arteaga-Cardona F, Gutiérrez-García E, Hidalgo-Tobón S et al (2016) Cell viability and MRI performance of highly efficient polyol-coated magnetic nanoparticles. J Nanopart Res. https://doi.org/10.1007/s11051-016-3646-0
12. Azizi M, Farahmandghavi F, Joghataei MT et al (2020) ChABC-loaded PLGA nanoparticles: a comprehensive study on biocompatibility, functional recovery, and axonal regeneration in animal model of spinal cord injury. Int J Pharm 577:119037. https://doi.org/10.1016/j.ijpharm.2020.119037
13. Barenholz Y (2012) Doxil®—the first FDA-approved nano-drug: lessons learned. J Control Release 160:117–134. https://doi.org/10.1016/j.jconrel.2012.03.020

14. Barui AK, Oh JY, Jana B et al (2020) Cancer-targeted nanomedicine: overcoming the barrier of the protein corona. Adv Ther 3:1900124. https://doi.org/10.1002/adtp.201900124
15. Berry CC (2009) Progress in functionalization of magnetic nanoparticles for applications in biomedicine. J Phys D Appl Phys. https://doi.org/10.1088/0022-3727/42/22/224003
16. Bhandari R, Gupta P, Dziubla T, Hilt JZ (2016) Single step synthesis, characterization and applications of curcumin functionalized iron oxide magnetic nanoparticles. Mater Sci Eng C 67:59–64. https://doi.org/10.1016/j.msec.2016.04.093
17. Biosca A, Dirscherl L, Moles E et al (2019) An immunopegliposome for targeted antimalarial combination therapy at the nanoscale. Pharmaceutics 11:1–19. https://doi.org/10.3390/pharmaceutics11070341
18. Bisht R, Rupenthal ID (2018) PLGA nanoparticles for intravitreal peptide delivery: statistical optimization, characterization and toxicity evaluation. Pharm Dev Technol 23:324–333. https://doi.org/10.1080/10837450.2016.1240184
19. Biswas S, Dodwadkar NS, Deshpande PP, Torchilin VP (2012) Liposomes loaded with paclitaxel and modified with novel triphenylphosphonium-PEG-PE conjugate possess low toxicity, target mitochondria and demonstrate enhanced antitumor effects in vitro and in vivo. J Control Release 159:393–402. https://doi.org/10.1016/j.jconrel.2012.01.009
20. Bulbake U, Doppalapudi S, Kommineni N, Khan W (2017) Liposomal formulations in clinical use: an updated review. Pharmaceutics 9:1–33. https://doi.org/10.3390/pharmaceutics9020012
21. Bulte JWM (2009) In vivo MRI cell tracking: clinical studies. Am J Roentgenol 193:314–325. https://doi.org/10.2214/AJR.09.3107
22. Cai D, Fan J, Wang S et al (2018) Primary biocompatibility tests of poly(lactide-co-glycolide)(poly-L-orithine/fucoidan) core–shell nanocarriers. R Soc open Sci. https://doi.org/10.1098/rsos.180320
23. Changsan N, Nilkaeo A, Pungrassami P, Srichana T (2009) Monitoring safety of liposomes containing rifampicin on respiratory cell lines and in vitro efficacy against Mycobacterium bovis in alveolar macrophages. J Drug Target 17:751–762. https://doi.org/10.3109/10611860903079462
24. Charrois GJR, Allen TM (2003) Rate of biodistribution of STEALTH® liposomes to tumor and skin: influence of liposome diameter and implications for toxicity and therapeutic activity. Biochim Biophys Acta Biomembr 1609:102–108. https://doi.org/10.1016/S0005-2736(02)00661-2
25. Chimote G, Banerjee R (2010) In vitro evaluation of inhalable isoniazid-loaded surfactant liposomes as an adjunct therapy in pulmonary tuberculosis. J Biomed Mater Res Part B Appl Biomater 94:1–10. https://doi.org/10.1002/jbm.b.31608
26. Clichici S, Filip A (2015) In vivo assessment of nanomaterials toxicity. Nanomater Toxic Risk Assess. https://doi.org/10.5772/60707
27. Cortajarena AL, Ortega D, Ocampo SM et al (2014) Engineering iron oxide nanoparticles for clinical settings. Nanobiomedicine. https://doi.org/10.5772/58841
28. COVID-19-Vaccine-Tracker (2022) https://vac-lshtm.shinyapps.io/ncov_vaccine_landscape/. Accessed 29 July 2022
29. Cui S, Wang Y, Gong Y et al (2018) Correlation of the cytotoxic effects of cationic lipids with their headgroups. Toxicol Res (Camb) 7:473–479. https://doi.org/10.1039/c8tx00005k
30. Dailey LA, Jekel N, Fink L et al (2006) Investigation of the proinflammatory potential of biodegradable nanoparticle drug delivery systems in the lung. Toxicol Appl Pharmacol 215:100–108. https://doi.org/10.1016/j.taap.2006.01.016
31. Do JH, An J, Joun YS et al (2008) Cellular-uptake behavior of polymer nanoparticles into consideration of biosafety. Macromol Res 16:695–703. https://doi.org/10.1007/BF03218583
32. Dokka S, Toledo D, Shi X et al (2000) Oxygen radical-mediated pulmonary toxicity induced by some cationic liposomes. Pharm Res 17:521–525. https://doi.org/10.1023/A:1007504613351
33. Dos Reis LG, Lee WH, Svolos M et al (2019) Nanotoxicologic effects of PLGA nanoparticles formulated with a cell-penetrating peptide: searching for a safe pDNA delivery system for the lungs. Pharmaceutics. https://doi.org/10.3390/pharmaceutics11010012
34. Dwivedi S, Siddiqui MA, Farshori NN et al (2014) Synthesis, characterization and toxicological evaluation of iron oxide nanoparticles in human lung alveolar epithelial cells. Colloids Surfaces B Biointerfaces 122:209–215. https://doi.org/10.1016/j.colsurfb.2014.06.064
35. Elmowafy EM, Tiboni M, Soliman ME (2019) Biocompatibility, biodegradation and biomedical applications of poly(lactic acid)/poly(lactic-co-glycolic acid) micro and nanoparticles. Springer, Singapore
36. Eroğlu İ, İbrahim M (2020) Liposome–ligand conjugates: a review on the current state of art. J Drug Target 28:225–244. https://doi.org/10.1080/1061186X.2019.1648479
37. Estelrich J, Antònia Busquets M (2018) Iron oxide nanoparticles in photothermal therapy. Molecules. https://doi.org/10.3390/molecules23071567
38. Feng Q, Liu Y, Huang J et al (2018) Uptake, distribution, clearance, and toxicity of iron oxide nanoparticles with different sizes and coatings. Sci Rep 8:1–13. https://doi.org/10.1038/s41598-018-19628-z
39. Fredenberg S, Wahlgren M, Reslow M, Axelsson A (2011) The mechanisms of drug release in poly(lactic-co-glycolic acid)-based drug delivery systems—a review. Int J Pharm 415:34–52. https://doi.org/10.1016/j.ijpharm.2011.05.049
40. Gábelová A, El Yamani N, Alonso TI et al (2017) Fibrous shape underlies the mutagenic and carcinogenic potential of nanosilver while surface chemistry affects the biosafety of iron oxide nanoparticles. Mutagenesis 32:193–202. https://doi.org/10.1093/mutage/gew045
41. Gabizon AA, Tzemach D, Horowitz AT et al (2006) Reduced toxicity and superior therapeutic activity of a mitomycin C lipid-based prodrug incorporated in pegylated liposomes. Clin Cancer Res 12:1913–1920. https://doi.org/10.1158/1078-0432.CCR-05-1547
42. Gao Z, Ma T, Zhao E et al (2016) Small is smarter: nano MRI contrast agents—advantages and recent achievements. Small 12:556–576. https://doi.org/10.1002/smll.201502309
43. Gaumet M, Vargas A, Gurny R, Delie F (2008) Nanoparticles for drug delivery: the need for precision in reporting particle size parameters. Eur J Pharm Biopharm 69:1–9. https://doi.org/10.1016/j.ejpb.2007.08.001
44. Gholizadeh S, Kamps JAAM, Hennink WE, Kok RJ (2018) PLGA-PEG nanoparticles for targeted delivery of the mTOR/PI3kinase inhibitor dactolisib to inflamed endothelium. Int J Pharm 548:747–758. https://doi.org/10.1016/j.ijpharm.2017.10.032
45. Gonzalez Gomez A, Syed S, Marshall K, Hosseinidoust Z (2019) Liposomal Nanovesicles For Efficient Encapsulation Of Staphylococcal Antibiotics. ACS Omega 4:10866–10876. https://doi.org/10.1021/acsomega.9b00825
46. Gossmann R, Langer K, Mulac D (2015) New perspective in the formulation and characterization of didodecyldimethylammonium bromide (DMAB) stabilized poly(lactic-co-glycolic acid) (PLGA) nanoparticles. PLoS ONE 10:1–15. https://doi.org/10.1371/journal.pone.0127532
47. Gossmann R, Spek S, Langer K, Mulac D (2018) Didodecyldimethylammonium bromide (DMAB) stabilized poly(lactic-co-glycolic acid) (PLGA) nanoparticles: Uptake and cytotoxic potential in Caco-2 cells. J Drug Deliv Sci Technol 43:430–438. https://doi.org/10.1016/j.jddst.2017.11.002
48. Grabowski N, Hillaireau H, Vergnaud J et al (2013) Toxicity of surface-modified PLGA nanoparticles toward lung alveolar epithelial cells. Int J Pharm 454:686–694. https://doi.org/10.1016/j.ijpharm.2013.05.025
49. Gu L, Fang RH, Sailor MJ, Park JH (2012) In vivo clearance and toxicity of monodisperse iron oxide nanocrystals. ACS Nano 6:4947–4954. https://doi.org/10.1021/nn300456z
50. Guglielmi V, Carton F, Vattemi G et al (2019) Uptake and intracellular distribution of different types of nanoparticles in primary human myoblasts and myotubes. Int J Pharm 560:347–356. https://doi.org/10.1016/j.ijpharm.2019.02.017
51. Guo L, Chen B, Liu R et al (2015) Biocompatibility assessment of polyethylene glycol-poly L-lysine-poly lactic-co-glycolic acid nanoparticles in vitro and in vivo. J Nanosci Nanotechnol 15:3710–3719. https://doi.org/10.1166/jnn.2015.9509
52. Hagens WI, Oomen AG, de Jong WH et al (2007) What do we (need to) know about the kinetic properties of nanoparticles in the body? Regul Toxicol Pharmacol 49:217–229. https://doi.org/10.1016/j.yrtph.2007.07.006
53. Hare JI, Lammers T, Ashford MB et al (2017) Challenges and strategies in anti-cancer nanomedicine development: an industry perspective. Adv Drug Deliv Rev 108:25–38. https://doi.org/10.1016/j.addr.2016.04.025
54. He Z, Shi Z, Sun W et al (2016) Hemocompatibility of folic-acid-conjugated amphiphilic PEG-PLGA copolymer nanoparticles for

co-delivery of cisplatin and paclitaxel: treatment effects for non-small-cell lung cancer. Tumor Biol 37:7809–7821. https://doi.org/10.1007/s13277-015-4634-1
55. He Z, Sun Y, Cao J, Duan Y (2016) Degradation behavior and biosafety studies of the mPEG-PLGA-PLL copolymer. Phys Chem Chem Phys 18:11986–11999. https://doi.org/10.1039/c6cp00767h
56. He Z, Sun Y, Wang Q et al (2015) Degradation and bio-safety evaluation of mPEG-PLGA-PLL copolymer-prepared nanoparticles. J Phys Chem C 119:3348–3362. https://doi.org/10.1021/jp510183s
57. Hong SC, Lee JH, Lee J et al (2011) Subtle cytotoxicity and genotoxicity differences in superparamagnetic iron oxide nanoparticles coated with various functional groups. Int J Nanomed 6:3219–3231
58. Hoskins C, Cuschieri A, Wang L (2012) The cytotoxicity of polycationic iron oxide nanoparticles: common endpoint assays and alternative approaches for improved understanding of cellular response mechanism. J Nanobiotechnol 10:1–11. https://doi.org/10.1186/1477-3155-10-15
59. Hu X, Sun A, Kang W, Zhou Q (2017) Strategies and knowledge gaps for improving nanomaterial biocompatibility. Environ Int 102:177–189. https://doi.org/10.1016/j.envint.2017.03.001
60. Huang WC, Deng B, Lin C et al (2018) A malaria vaccine adjuvant based on recombinant antigen binding to liposomes. Nat Nanotechnol 13:1174–1181. https://doi.org/10.1038/s41565-018-0271-3
61. Igartúa DE, Azcona PL, Martinez CS et al (2018) Folic acid magnetic nanotheranostics for delivering doxorubicin: toxicological and biocompatibility studies on Zebrafish embryo and larvae. Toxicol Appl Pharmacol 358:23–34. https://doi.org/10.1016/j.taap.2018.09.009
62. Inglut CT, Sorrin AJ, Kuruppu T et al (2020) Immunological and toxicological considerations for the design of liposomes. Nanomaterials. https://doi.org/10.3390/nano10020190
63. Ivask A, Kurvet I, Kasemets K et al (2014) Size-dependent toxicity of silver nanoparticles to bacteria, yeast, algae, crustaceans and mammalian cells in vitro. PLoS ONE. https://doi.org/10.1371/journal.pone.0102108
64. Joon SC, Lee EJ, Jang HS, Park JS (2001) New cationic liposomes for gene transfer into mammalian cells with high efficiency and low toxicity. Bioconjug Chem 12:108–113. https://doi.org/10.1021/bc000081o
65. Joris F, Manshian BB, Peynshaert K et al (2013) Assessing nanoparticle toxicity in cell-based assays: influence of cell culture parameters and optimized models for bridging the in vitro-in vivo gap. Chem Soc Rev 42:8339–8359. https://doi.org/10.1039/c3cs60145e
66. Kamaly N, Yameen B, Wu J, Farokhzad OC (2016) Degradable controlled-release polymers and polymeric nanoparticles: mechanisms of controlling drug release. Chem Rev 116:2602–2663. https://doi.org/10.1021/acs.chemrev.5b00346
67. Kansara K, Patel P, Shukla RK et al (2018) Synthesis of biocompatible iron oxide nanoparticles as a drug delivery vehicle. Int J Nanomed 13:79–82. https://doi.org/10.2147/IJN.S124708
68. Kargozar S, Mozafari M (2018) Nanotechnology and nanomedicine: start small, think big. Mater Today Proc 5:15492–15500. https://doi.org/10.1016/j.matpr.2018.04.155
69. Kim DH (2018) Image-guided cancer nanomedicine. J Imaging 4:1–7. https://doi.org/10.3390/jimaging4010018
70. Kim YS, Park JS, Park M et al (2018) PLGA nanoparticles with multiple modes are a biologically safe nanocarrier for mammalian development and their offspring. Biomaterials 183:43–53. https://doi.org/10.1016/j.biomaterials.2018.08.042
71. Knudsen KB, Northeved H, Pramod Kumar EK et al (2015) In vivo toxicity of cationic micelles and liposomes. Nanomed Nanotechnol Biol Med 11:467–477. https://doi.org/10.1016/j.nano.2014.08.004
72. Kolosnjaj-Tabi J, Just J, Hartman KB et al (2015) Anthropogenic carbon nanotubes found in the airways of parisian children. EBioMedicine 2:1697–1704. https://doi.org/10.1016/j.ebiom.2015.10.012
73. Krucinska I, Zywicka B, Komisarczyk A et al (2017) Biological properties of low-toxicity PLGA and PLGA/PHB fibrous nanocomposite implants for osseous tissue regeneration. Part I: evaluation of potential biotoxicity. Molecules 22:1–25. https://doi.org/10.3390/molecules22122092
74. Kuang Y, Liu J, Liu Z, Zhuo R (2012) Cholesterol-based anionic long-circulating cisplatin liposomes with reduced renal toxicity. Biomaterials 33:1596–1606. https://doi.org/10.1016/j.biomaterials.2011.10.081
75. Kumar V, Sharma N, Maitra SS (2017) In vitro and in vivo toxicity assessment of nanoparticles. Int Nano Lett 7:243–256. https://doi.org/10.1007/s40089-017-0221-3
76. Lamichhane N, Udayakumar TS, D'Souza WD et al (2018) Liposomes: clinical applications and potential for image-guided drug delivery. Molecules 23:1–17. https://doi.org/10.3390/molecules23020288
77. Lee JH, Ju JE, Il KB et al (2014) Rod-shaped iron oxide nanoparticles are more toxic than sphere-shaped nanoparticles to murine macrophage cells. Environ Toxicol Chem 33:2759–2766. https://doi.org/10.1002/etc.2735
78. Li L, Jiang W, Luo K et al (2013) Superparamagnetic iron oxide nanoparticles as MRI contrast agents for non-invasive stem cell labeling and tracking. Theranostics 3:595–615. https://doi.org/10.7150/thno.5366
79. Li M, Al-Jamal KT, Kostarelos K, Reineke J (2010) Physiologically based pharmacokinetic modeling of nanoparticles. ACS Nano 4:6303–6317. https://doi.org/10.1021/nn1018818
80. Li X, Liu W, Sun L et al (2015) Effects of physicochemical properties of nanomaterials on their toxicity. J Biomed Mater Res Part A 103:2499–2507. https://doi.org/10.1002/jbm.a.35384
81. Li X, Wang L, Fan Y et al (2012) Biocompatibility and toxicity of nanoparticles and nanotubes. J Nanomater. https://doi.org/10.1155/2012/548389
82. Li Y, Liu J, Zhong Y et al (2011) Biocompatibility of Fe_3O_4@Au composite magnetic nanoparticles in vitro and in vivo. Int J Nanomed 6:2805–2819. https://doi.org/10.2147/ijn.s24596
83. Longmire M, Choyke PL, Kobayashi H (2008) Clearance properties of nano-sized particles and molecules as imaging agents: considerations and caveats. Nanomedicine 3:703–717. https://doi.org/10.2217/17435889.3.5.703
84. Luzala MM, Muanga CK, Kyana J et al (2022) A critical review of the antimicrobial and antibiofilm activities of green-synthesized plant-based metallic nanoparticles. Nanomaterials 12:1841. https://doi.org/10.3390/nano12111841
85. Mahdavinia GR, Etemadi H (2019) Surface modification of iron oxide nanoparticles with κ-carrageenan/carboxymethyl chitosan for effective adsorption of bovine serum albumin. Arab J Chem 12:3692–3703. https://doi.org/10.1016/j.arabjc.2015.12.002
86. Makadia HK, Siegel SJ (2011) Poly lactic-co-glycolic acid (PLGA) as biodegradable controlled drug delivery carrier. Polymers 3:1377–1397. https://doi.org/10.3390/polym3031377
87. Malhotra N, Lee JS, Liman RAD et al (2020) Potential toxicity of iron oxide magnetic nanoparticles: a review. Molecules 25:1–26. https://doi.org/10.3390/molecules25143159
88. Malvindi MA, De Matteis V, Galeone A et al (2014) Toxicity assessment of silica coated iron oxide nanoparticles and biocompatibility improvement by surface engineering. PLoS ONE 9:1–11. https://doi.org/10.1371/journal.pone.0085835
89. Mao J, Liu S, Ai M et al (2017) A novel melittin nano-liposome exerted excellent anti-hepatocellular carcinoma efficacy with better biological safety. J Hematol Oncol 10:4–7. https://doi.org/10.1186/s13045-017-0442-y
90. Martins C, Sousa F, Araújo F, Sarmento B (2018) Functionalizing PLGA and PLGA derivatives for drug delivery and tissue regeneration applications. Adv Healthc Mater 7:1–24. https://doi.org/10.1002/adhm.201701035
91. Meng H, Wei L, Kam WL et al (2018) Walking the line: the fate of nanomaterials at biological barriers. Biomaterials 174:41–53. https://doi.org/10.1016/j.biomaterials.2018.04.056.Walking
92. Mohammadi H, Hafezi M, Hesaraki S, Sepantafar MM (2015) Preparation and characterization of Sr–Ti–hardystonite (Sr–Ti–HT) nanocomposite for bone repair application. Nanomed J 2:203–210. https://doi.org/10.7508/nmj
93. Moraes Moreira Carraro TC, Altmeyer C, Maissar Khalil N, Mara Mainardes R (2017) Assessment of in vitro antifungal efficacy and in vivo toxicity of Amphotericin B-loaded PLGA and PLGA-PEG blend nanoparticles. J Mycol Med 27:519–529. https://doi.org/10.1016/j.mycmed.2017.07.004
94. Mura S, Hillaireau H, Nicolas J et al (2011) Influence of surface charge on the potential toxicity of PLGA nanoparticles towards Calu-3 cells. Int J Nanomed 6:2591–2605. https://doi.org/10.2147/ijn.s24552

95. Naha PC, Liu Y, Hwang G et al (2019) Dextran-coated iron oxide nanoparticles as biomimetic catalysts for localized and pH-activated biofilm disruption. ACS Nano 13:4960–4971. https://doi.org/10.1021/acsnano.8b08702
96. Navarro SM, Morgan TW, Astete CE et al (2016) Biodistribution and toxicity of orally administered poly(lactic-co-glycolic) acid nanoparticles to F344 rats for 21 days. Nanomedicine 11:1653–1669. https://doi.org/10.2217/nnm-2016-0022
97. Ni W, Li Z, Liu Z et al (2019) Dual-targeting nanoparticles: codelivery of curcumin and 5-fluorouracil for synergistic treatment of hepatocarcinoma. J Pharm Sci 108:1284–1295. https://doi.org/10.1016/j.xphs.2018.10.042
98. Nkanga CI, Bapolisi AM, Okafor NI, Krause RWM (2019) General perception of liposomes: formation, manufacturing and applications
99. Nkanga CI, Fisch A, Rad-Malekshahi M et al (2020) Clinically established biodegradable long acting injectables: an industry perspective. Adv Drug Deliv Rev 167:19–46. https://doi.org/10.1016/j.addr.2020.11.008
100. Nkanga CI, Krause RWM (2019) Encapsulation of isoniazid-conjugated phthalocyanine-in-cyclodextrin-in-liposomes using heating method. Sci Rep 9:11485. https://doi.org/10.1038/s41598-019-47991-y
101. Nkanga CI, Roth M, Walker RB et al (2020) Co-loading of Isoniazid-grafted phthalocyanine-in-cyclodextrin and rifampicin in crude soybean lecithin liposomes: formulation, spectroscopic and biological characterization. J Biomed Nanotechnol 16:14–28. https://doi.org/10.1166/jbn.2020.2880
102. Owens DE, Peppas NA (2006) Opsonization, biodistribution, and pharmacokinetics of polymeric nanoparticles. Int J Pharm 307:93–102. https://doi.org/10.1016/j.ijpharm.2005.10.010
103. Pan J, Sun SK, Wang Y et al (2015) Facile preparation of hyaluronic acid and transferrin co-modified Fe_3O_4 nanoparticles with inherent biocompatibility for dual-targeting magnetic resonance imaging of tumors in vivo. Dalt Trans 44:19836–19843. https://doi.org/10.1039/c5dt02486b
104. Pandit J, Sultana Y, Aqil M (2017) Chitosan-coated PLGA nanoparticles of bevacizumab as novel drug delivery to target retina: optimization, characterization, and in vitro toxicity evaluation. Artif Cells Nanomed Biotechnol 45:1397–1407. https://doi.org/10.1080/21691401.2016.1243545
105. Park K, Skidmore S, Hadar J et al (2019) Injectable, long-acting PLGA formulations: analyzing PLGA and understanding microparticle formation. J Control Release 304:125–134. https://doi.org/10.1016/j.jconrel.2019.05.003
106. Park YC, Smith JB, Pham T et al (2014) Effect of PEG molecular weight on stability, T2 contrast, cytotoxicity, and cellular uptake of superparamagnetic iron oxide nanoparticles (SPIONs). Colloids Surfaces B Biointerfaces 119:106–114. https://doi.org/10.1016/j.colsurfb.2014.04.027
107. Patel S, Jana S, Chetty R et al (2019) Toxicity evaluation of magnetic iron oxide nanoparticles reveals neuronal loss in chicken embryo. Drug Chem Toxicol 42:1–8. https://doi.org/10.1080/01480545.2017.1413110
108. Patil-Gadhe AA, Kyadarkunte AY, Pereira M et al (2014) Rifapentine-proliposomes for inhalation: in vitro and in vivo toxicity. Toxicol Int 21:275–282. https://doi.org/10.4103/0971-6580.155361
109. Paul PS, Cho JY, Wu Q et al (2022) Unconjugated PLGA nanoparticles attenuate temperature-dependent β-amyloid aggregation and protect neurons against toxicity: implications for Alzheimer's disease pathology. J Nanobiotechnol 20:1–26. https://doi.org/10.1186/s12951-022-01269-0
110. Paul S, Rao S, Kohan R et al (2013) Poractant alfa versus beractant for respiratory distress syndrome in preterm infants: a retrospective cohort study. J Paediatr Child Health 49:839–844. https://doi.org/10.1111/jpc.12300
111. Pereverzeva E, Treschalin I, Treschalin M et al (2019) Toxicological study of doxorubicin-loaded PLGA nanoparticles for the treatment of glioblastoma. Int J Pharm 554:161–178. https://doi.org/10.1016/j.ijpharm.2018.11.014
112. Pongrac IM, Pavičić I, Milić M et al (2016) Oxidative stress response in neural stem cells exposed to different superparamagnetic iron oxide nanoparticles. Int J Nanomed 11:1701–1715. https://doi.org/10.2147/IJN.S102730
113. Portilla S, Fernández L, Gutiérrez D et al (2020) Encapsulation of the antistaphylococcal endolysin LysRODI in pH-sensitive liposomes. Antibiotics. https://doi.org/10.3390/antibiotics9050242
114. Prabhu S, Mutalik S, Rai S et al (2015) PEGylation of superparamagnetic iron oxide nanoparticle for drug delivery applications with decreased toxicity: an in vivo study. J Nanopart Res. https://doi.org/10.1007/s11051-015-3216-x
115. Qiao R, Yang C, Gao M (2009) Superparamagnetic iron oxide nanoparticles: from preparations to in vivo MRI applications. J Mater Chem 19:6274–6293. https://doi.org/10.1039/b902394a
116. Raju HB, Hu Y, Vedula A et al (2011) Evaluation of magnetic micro- and nanoparticle toxicity to ocular tissues. PLoS ONE. https://doi.org/10.1371/journal.pone.0017452
117. Ramot Y, Haim-Zada M, Domb AJ, Nyska A (2016) Biocompatibility and safety of PLA and its copolymers. Adv Drug Deliv Rev 107:153–162. https://doi.org/10.1016/j.addr.2016.03.012
118. Rudokas M, Najlah M, Alhnan MA, Elhissi A (2016) Liposome delivery systems for inhalation: a critical review highlighting formulation issues and anticancer applications. Med Princ Pract 25:60–72. https://doi.org/10.1159/000445116
119. Ruess D, Grau S, Hoevels M, Treuer Harald GR (2015) Application of nanothermw by stereotactic guidance: a technical note. Neuro Oncol 17:214–220. https://doi.org/10.1093/neuonc/nov061.154
120. Ryabchikova E (2021) Advances in nanomaterials in biomedicine. Nanomaterials 11:1–5. https://doi.org/10.3390/nano11010118
121. Sun S, Zeng H, Robinson DB, Raoux S, Rice PM, Wang SX, Li G (2004) Monodisperse MFe_2O_4 (M) Fe Co, Mn) nanoparticles shouheng. J Am Chem Soc 126:273–279
122. Savage DT, Hilt JZ, Dziubla TD (2019) In vitro methods for assessing nanoparticle toxicity. Methods Mol Biol 1894:1–29. https://doi.org/10.1007/978-1-4939-8916-4_1
123. Semete B, Booysen L, Lemmer Y et al (2010) In vivo evaluation of the biodistribution and safety of PLGA nanoparticles as drug delivery systems. Nanomed Nanotechnol Biol Med 6:662–671. https://doi.org/10.1016/j.nano.2010.02.002
124. Shams F, Golchin A, Azari A et al (2022) Nanotechnology-based products for cancer immunotherapy. Mol Biol Rep 49:1389–1412. https://doi.org/10.1007/s11033-021-06876-y
125. Shen X, Wang Y, Xi L et al (2019) Biocompatibility and paclitaxel/cisplatin dual-loading of nanotubes prepared from poly(ethylene glycol)-polylactide-poly(ethylene glycol) triblock copolymers for combination cancer therapy. Saudi Pharm J 27:1025–1035. https://doi.org/10.1016/j.jsps.2019.08.005
126. Shi L, Wu X, Li T et al (2022) An esterase-activatable prodrug formulated liposome strategy: potentiating the anticancer therapeutic efficacy and drug safety. Nanoscale Adv 4:952–966. https://doi.org/10.1039/d1na00838b
127. Silva AH, Lima E, Mansilla MV et al (2016) Superparamagnetic iron-oxide nanoparticles mPEG350- and mPEG2000-coated: cell uptake and biocompatibility evaluation. Nanomed Nanotechnol Biol Med 12:909–919. https://doi.org/10.1016/j.nano.2015.12.371
128. Silva ATCR, Cardoso BCO, Silva MESR et al (2015) Synthesis, characterization, and study of PLGA copolymer in vitro degradation. J Biomater Nanobiotechnol 06:8–19. https://doi.org/10.4236/jbnb.2015.61002
129. Singh N, Jenkins GJS, Asadi R, Doak SH (2010) Potential toxicity of superparamagnetic iron oxide nanoparticles (SPION). Nano Rev 1:5358. https://doi.org/10.3402/nano.v1i0.5358
130. Souza ACO, Nascimento AL, de Vasconcelos NM et al (2015) Activity and in vivo tracking of amphotericin B loaded PLGA nanoparticles. Eur J Med Chem 95:267–276. https://doi.org/10.1016/j.ejmech.2015.03.022
131. Stepien G, Moros M, Pérez-Hernández M et al (2018) Effect of surface chemistry and associated protein corona on the long-term biodegradation of iron oxide nanoparticles in Vivo. ACS Appl Mater Interfaces 10:4548–4560. https://doi.org/10.1021/acsami.7b18648
132. Stevanović M, Maksin T, Petković J et al (2009) An innovative, quick and convenient labeling method for the investigation of pharmacological behavior and the metabolism of poly(DL-lactide-co-glycolide) nanospheres. Nanotechnology. https://doi.org/10.1088/0957-4484/20/33/335102
133. Sukhanova A, Bozrova S, Sokolov P et al (2018) Dependence of nanoparticle toxicity on their physical and chemical properties. Nanoscale Res Lett. https://doi.org/10.1186/s11671-018-2457-x

134. Sun T, Zhang YS, Pang B et al (2014) Engineered nanoparticles for drug delivery in cancer therapy. Angew Chemie Int Ed 53:12320–12364. https://doi.org/10.1002/anie.201403036
135. Syama K, Jakubek ZJ, Chen S et al (2022) Development of lipid nanoparticles and liposomes reference materials(II): cytotoxic profiles. Sci Rep 12:1–11. https://doi.org/10.1038/s41598-022-23013-2
136. Szebeni J, Bedocs P, Rozsnyay Z et al (2012) Liposome-induced complement activation and related cardiopulmonary distress in pigs: factors promoting reactogenicity of Doxil and Am Bisome. Nanomed Nanotechnol Biol Med 8:176–184. https://doi.org/10.1016/j.nano.2011.06.003
137. Tacar O, Sriamornsak P, Dass CR (2013) Doxorubicin: an update on anticancer molecular action, toxicity and novel drug delivery systems. J Pharm Pharmacol 65:157–170. https://doi.org/10.1111/j.2042-7158.2012.01567.x
138. Tang C, Yin D, Liu T et al (2022) Maleimide-functionalized liposomes: prolonged retention and enhanced efficacy of doxorubicin in breast cancer with low systemic toxicity. Molecules. https://doi.org/10.3390/molecules27144632
139. Theodoulou M, Hudis C (2004) Cardiac profiles of liposomal anthracyclines: greater cardiac safety versus conventional doxorubicin? Cancer 100:2052–2063. https://doi.org/10.1002/cncr.20207
140. Utreja P, Jain S, Tiwary AK (2012) Evaluation of biosafety and intracellular uptake of cremophor EL free paclitaxel elastic liposomal formulation. Drug Deliv 19:11–20. https://doi.org/10.3109/10717544.2011.621990
141. Vasanawala SS, Nguyen KL, Hope MD et al (2016) Safety and technique of ferumoxytol administration for MRI. Magn Reson Med 75:2107–2111. https://doi.org/10.1002/mrm.26151
142. Villanueva-Bermejo D, Temelli F (2020) Optimization of coenzyme Q10 encapsulation in liposomes using supercritical carbon dioxide. J CO2 Util 38:68–76. https://doi.org/10.1016/j.jcou.2020.01.011
143. Wang L, Cao J, Li C et al (2022) Efficacy and safety of mitoxantrone hydrochloride liposome injection in Chinese patients with advanced breast cancer: a randomized, open-label, active-controlled, single-center, phase II clinical trial. Invest New Drugs 40:330–339. https://doi.org/10.1007/s10637-021-01182-7
144. Wang L, Xing H, Guo S et al (2023) Negatively charged phospholipids doped liposome delivery system for mRNA with high transfection efficiency and low cytotoxicity. Drug Deliv. https://doi.org/10.1080/10717544.2023.2219869
145. Wicki A, Witzigmann D, Balasubramanian V, Huwyler J (2015) Nanomedicine in cancer therapy: challenges, opportunities, and clinical applications. J Control Release 200:138–157. https://doi.org/10.1016/j.jconrel.2014.12.030
146. Witika BA, Makoni PA, Matafwali SK et al (2020) Biocompatibility of biomaterials for nanoencapsulation: current approaches. Nanomaterials 10:1649. https://doi.org/10.3390/nano10091649
147. Wu M, Gu L, Gong Q et al (2017) Strategies to reduce the intracellular effects of iron oxide nanoparticle degradation. Nanomedicine 12:555–570. https://doi.org/10.2217/nnm-2016-0328
148. Wu Q, Karthivashan G, Nakhaei-Nejad M et al (2022) Native PLGA nanoparticles regulate APP metabolism and protect neurons against β-amyloid toxicity: potential significance in Alzheimer's disease pathology. Int J Biol Macromol 219:1180–1196. https://doi.org/10.1016/j.ijbiomac.2022.08.148
149. Xi J, Qian X, Qian K et al (2015) Au nanoparticle-coated, PLGA-based hybrid capsules for combined ultrasound imaging and HIFU therapy. J Mater Chem B 3:4213–4220. https://doi.org/10.1039/c5tb00200a
150. Xia DL, Chen YP, Chen C et al (2015) Comparative study of biosafety, DNA, and chromosome damage of different-materials-modified Fe_3O_4 in rats. Appl Biochem Biotechnol 177:1069–1082. https://doi.org/10.1007/s12010-015-1797-6
151. Xiang Y, Bai Z, Zhang S et al (2017) Lead adsorption, anticoagulation and in vivo toxicity studies on the new magnetic nanomaterial Fe_3O_4@SiO_2@DMSA as a hemoperfusion adsorbent. Nanomed Nanotechnol Biol Med 13:1341–1351. https://doi.org/10.1016/j.nano.2017.01.007
152. Xie W, Guo Z, Gao F et al (2018) Shape-, size-and structure-controlled synthesis and biocompatibility of iron oxide nanoparticles for magnetic theranostics. Theranostics 8:3284–3307. https://doi.org/10.7150/thno.25220
153. Xiong S, Yu S, George H, Damoiseaux R et al (2013) Size influences the cytotoxicity of poly(lactic-co-glycolic acid) (PLGA) and titanium dioxide (TiO_2) nanoparticles. Arch Toxicol 87:1075–1086. https://doi.org/10.1007/s00204-012-0938-8.Size
154. Yang Y, Qin Z, Zeng W et al (2017) Toxicity assessment of nanoparticles in various systems and organs. Nanotechnol Rev 6:279–289. https://doi.org/10.1515/ntrev-2016-0047
155. Yarjanli Z, Ghaedi K, Esmaeili A et al (2017) Iron oxide nanoparticles may damage to the neural tissue through iron accumulation, oxidative stress, and protein aggregation. BMC Neurosci 18:1–12. https://doi.org/10.1186/s12868-017-0369-9
156. Yildirimer L, Thanh NTK, Loizidou M, Seifalian AM (2011) Toxicological considerations of clinically applicable nanoparticles. Nano Today 6:585–607. https://doi.org/10.1016/j.nantod.2011.10.001
157. Yin X, Luo L, Li W et al (2019) A cabazitaxel liposome for increased solubility, enhanced antitumor effect and reduced systemic toxicity. Asian J Pharm Sci 14:658–667. https://doi.org/10.1016/j.ajps.2018.10.004
158. Yoganandham Suman T, Li W-G, Pei D-S (2020) Toxicity of metal oxide nanoparticles. Nanotoxicity. https://doi.org/10.1016/b978-0-12-819943-5.00005-1
159. Zhong H, Chan G, Hu Y et al (2018) A comprehensive map of FDA-approved pharmaceutical products. Pharmaceutics 10:1–19. https://doi.org/10.3390/pharmaceutics10040263

Publisher's Note